The Otto Glacier on Borah Peak, Lost River Range, Custer County, Idaho:

Reconnaissance Survey Finds Further Evidence for Active Glacier

Watershed Monitoring Program 2015

Salmon-Challis National Forest

Prepared by

Joshua Keeley

Mathew Warbritton

ABSTRACT

In 1974, Idaho's only documented active glacier was discovered after an investigation of the perennial body of snow and ice on the north face of Borah Peak (12,662 feet). The glacier was named the Otto glacier after its discoverer, who documented ice movement by observing active crevasses and rotated icicles therein. Informal monitoring of the glacier over the following 41 years has determined a general stasis of the ice mass, observing only minor fluctuations from year to year.

The 2015 United States Forest Service (USFS) reconnaissance survey of the Otto glacier took place on September 24, during which key features of the perennial ice were assessed, measured, and sampled. Our survey confirmed the continued presence of the perennial ice mass originally identified in 1974, and concluded that the ice mass is indeed a glacier that continues to move under its own weight, based on measurements described herein in conjunction with results from the initial investigations in the 1970's. The glacier is classified as a semi-covered clean-ice glacier based on the thin surficial cover of rock debris over two-thirds of the glacier's extent. Total area from bergschrund crevasse to the toe-slope of the terminal moraine is 0.1 km^2 (25 acres). Remote sensing techniques using historical Google Earth imagery over a three-year period (2011-2014) has detected between 50 and 200 cm of *down*-slope movement per year. In addition, theoretical internal strain rates of the ice calculated using Glen-Nye flow law parameters independently predict this velocity.

Deuterium and oxygen isotopes were obtained from 4 ice samples and 1 meltwater pond downstream of the glacier in order to characterize the hydrologic cycle at the glacier. Delta deuterium (δ^2H) ranges from -130.06 to -118.59 VSMOW ‰ and delta-O-18 ($\delta^{18}O$) range from -17.17 to -16.05 VSMOW ‰. A comparison between Otto glacier values and published snow and rain data from the northern Rocky Mountains shows that the ice has integrated isotopically heavy (higher values) summer precipitation with isotopically light (lower values) winter precipitation. The processes that may have produced the isotopic mixing are winter snow removal by wind and percolation of summer rain through the perennial snowpack. A preliminary comparison with current weather data suggests that the Borah Peak area receives higher rainfall and higher temperatures than other Rocky Mountain glaciers like the Schoolroom and Fremont glaciers in Wyoming. This suggests that the dominant factor contributing to glacier preservation is the near complete shading it receives from the north face of Borah Peak.

PURPOSE

The objective of the project was to obtain physical evidence and documentation of the current state and designation of the perennial ice mass on the north face of Borah Peak. The work was requested by the Regional office in an effort to update United States Geological Survey (USGS) mapping.

Reconnaissance mapping and surveying of the proposed Otto glacier (named after its discoverer, Bruce Otto) was conducted in order to determine whether the icepack satisfies the criteria of a glacier: (1) Perennial snowpack leading to (2) formation of stratified ice that (3) moves *down*-slope by basal slip and internal deformation. Ice samples were taken to characterize the hydrologic cycle of the glacier. Additionally, we considered classifications of debris-mantled glaciers and rock glaciers based on the thickness of rock debris that covers the ice, and the percentage of ice within the rocky portion of the moraine, respectively.

Although the feature has been well documented and classified as a glacier by Otto (1975; 1977), the icepack is currently not listed by the USGS's National Hydrography Database. We are thus undertaking this reconnaissance study primarily in response to public and academic inquiry, and secondly because of the scientific importance and climatic implications of potentially listing Idaho's first (and perhaps only) active glacier in a national database.

Whereas there are currently no nationally recognized active glaciers in Idaho, numerous glaciers are present in nearby states of Wyoming (Teton and Wind River ranges) and Montana (Glacier National Park). Glacier development is dependent upon several interacting climatic, geographic, and topographic parameters (e.g., snow precipitation, topography, aspect, latitude, regional climate and local weather, etc.). Each region listed above has unique contributing factors that lead to glacier growth and preservation. For example, the dominant contributing factor of glacier growth in the Teton Range is its springtime snow precipitation, which increases snowpack during an otherwise melt season while also reducing solar insolation (Reynolds, 2011).

INTRODUCTION

An Introduction to Glaciers and Glacial Processes

A glacier is defined as a perennial mass of land ice formed by the recrystallization of snow that accumulates stress leading to the *down*-slope or outward motion of the ice mass. Glaciers are classified based on the landform that they occupy (cirque glaciers, valley glaciers, piedmont glaciers, etc.) and range from small ($1.0X10^{-1}km^2$) to extremely large (up to $2X10^4km^2$) depending on climatic and geographic factors. Alpine glaciers (cirque and valley glaciers) are further subdivided into clean-ice

glaciers, debris-covered glaciers, and rock glaciers depending on the thickness of their debris mantle and the estimated ice-to-rock ratio within (Janke et al., 2015). For the purposes of this report, we focus on alpine glaciers in the northern Rocky Mountains of Idaho, Wyoming and Montana.

Alpine glaciers usually originate in cirques and may move *down*-slope in the valley below. The extent to how far they move is a function of glacial budget or mass balance. Mass balance is the difference between total snow accumulation (which leads to compaction and eventual ice deposition) and ablation (the combined process by which the glacier wastes, melting + sublimation). All glaciers have an accumulation zone and an ablation zone separated by an equilibrium line, which is usually marked by the fresh snowline. A glacier will move *down*-slope if accumulation exceeds ablation and alternatively, will recede upslope if ablation exceeds accumulation. Mechanically, it moves by basal slip (rigid slip between the ice and underlying rock) and internal deformation. The rate at which ice internally deforms, or is strained, depends on the physical properties of ice (e.i., viscosity, density, thickness) and the amount of force, or stress, applied. Stress is the product of gravity and the ice's mass and depends greatly on the slope of bedrock on which the glacier resides and the friction between ice and rock.

Whether or not the *down*-slope terminus of the glacier is advancing or receding, sediment deposition is constantly occurring. As the glacier moves, it grinds, scours, and depresses the rock beneath it often generating a U-shaped valley. The eroded rock and sediment load of variably-sized silt and clay (commonly called rock flour when referring to glaciers) to large boulders and blocks is transported within the ice and on top of the glacier toward the margins. Some debris at the toe of the glacier may even by "bulldozed" into a terminal moraine. Even if the glacier is static (accumulation = ablation), sediment is transported within the ice via internal deformation to the toe and sides of the glacier much like a conveyor belt. In this way, end moraines and lateral moraines may continue to receive sediment regardless of glacier growth.

Pleistocene–Holocene Glaciations in the Rocky Mountains and Idaho

Glacial moraines and U-shaped valleys in the Northern Rocky Mountains are a testament to at least three glacial advances during the Pleistocene Epoch between 150,000 and 10,000 years before present (150–10 ka, or kilo-annum) (Pierce, 2003; Thackray et al., 2004). Smaller and more rare Holocene moraines are restricted to high mountain cirques. Geologists have used a multitude of methods to date these advances; measuring concentrations of cosmogenic nuclides (^{10}Be and ^{26}Al) on recently exposed rocks; radiogenic age-dating of carbonate rinds of carbonate rocks on moraines and

igneous rocks that cross cut or overlay glacial advances; carbon-dating glacial beds in lakes; and tree ring analyses in recently deglaciated valleys (to name a few).

The most pronounced glacial advance in the Rocky Mountains is the Bull Lake glaciation, named after the lake in Wyoming (Blackwelder, 1915). The older broad-crested Bull Lake moraines outside of West Yellowstone, Wyoming, were dated to 150–130 ka (Pierce et al, 1976; Pierce, 2003 and references therein), which correlates to the more widespread Illinoian glaciation of the Laurentide Ice Sheet of North America. The following Pinedale advance is named after the pronounced moraines near Pinedale, Wyoming, deposited by glaciers that originated in the Wind River Range (Figs. 1-2). These younger and more sharp-crested moraines have been dated between 25–14 ka (Gosse et al., 1995; Pierce et al., 2014), correlating to the Wisconsinan glaciation of the Laurentide Ice Sheet. In the Sawtooth Mountains, near Stanley, ID, Thackray et al. (2004) carbon-dated glacial lake sediments which yielded a late-glacial age of 14 ka, similar to glacial deposits near McCall, ID (Colman and Pierce, 1984). Slightly younger ages come out of the White Cloud Range, where volcanic ashes deposited in a glacial lake setting were dated to 14–11 ka (Cotter et al., 1986; Bloomfield, 1983).

Evidence of glaciation and deglaciation in Idaho is prevalent (Fig. 1). Evidence for direct ice contact includes glacial moraines, glacial striations, and sculpted arêtes and horns on high mountain ranges of the Sawtooth, Pioneer, and Bitterroot mountains, and the Lemhi, Lost River, and Albion ranges. Evidence for the Columbian ice sheet also exists on the Idaho panhandle. Many active glaciers exist in the nearby Teton and Wind River Ranges, whereas rock glaciers have been documented in the adjacent Lemhi Range (Johnson et al., 2007) (Figs. 2 and 3). Rock glaciers are defined as having a thicker surface rock layer than debris-covered glaciers that have a mixture of rock and ice at depth (Janke et al., 2015). Glacial process that occur near or away from the ice margin leave periglacial features, like terraces in incised valleys, kame terraces, glacial lakes, and glacial flood scours. Evidence for cataclysmic and glacial outwash floods like the Bonneville and Missoula from their respective glacial lakes occurs throughout the Snake River and Columbia River watersheds (Fig. 1).

Glacial striations, sculpted arêtes and horns, kame terraces, and moraines along in the Lost River Range in east-central Idaho are testament to one or more of the aforementioned glacial advances. Glacial features are particularly prominent at the outlet of Rock Creek near the Borah Peak trailhead. The large alluvial fan that extends into Lost River Valley from Rock Creek reflects the relatively small drainage of Rock Creek once had a much larger discharge. Similarly, the active Rock Creek channel is much broader than its current flow would indicate. Whereas the bottom portion of Rock Creek is V-shaped, incised by stream erosion over time, the central portion is U-shaped, clear evidence of glacial

sculpting (Fig. 4). These features, along with the observation of the perennial field of snow and ice on the north face of Borah led to the first direct investigation of the ice mass.

It is most likely that the Otto glacier represents a Holocene glacial pulse and possibly a remnant of the Little Ice Age (circa 1300–1850) (Luckman, 2000). Evidence suggests that prior to the Little Ice Age (LIA) much of the early Holocene was warmer than today (Oritz et al., 2000). If so, this glacier could have been greatly diminished after the Holocene warming event and then subsequently grown to a maximum during the LIA, only to be once again diminished over the last hundred years.

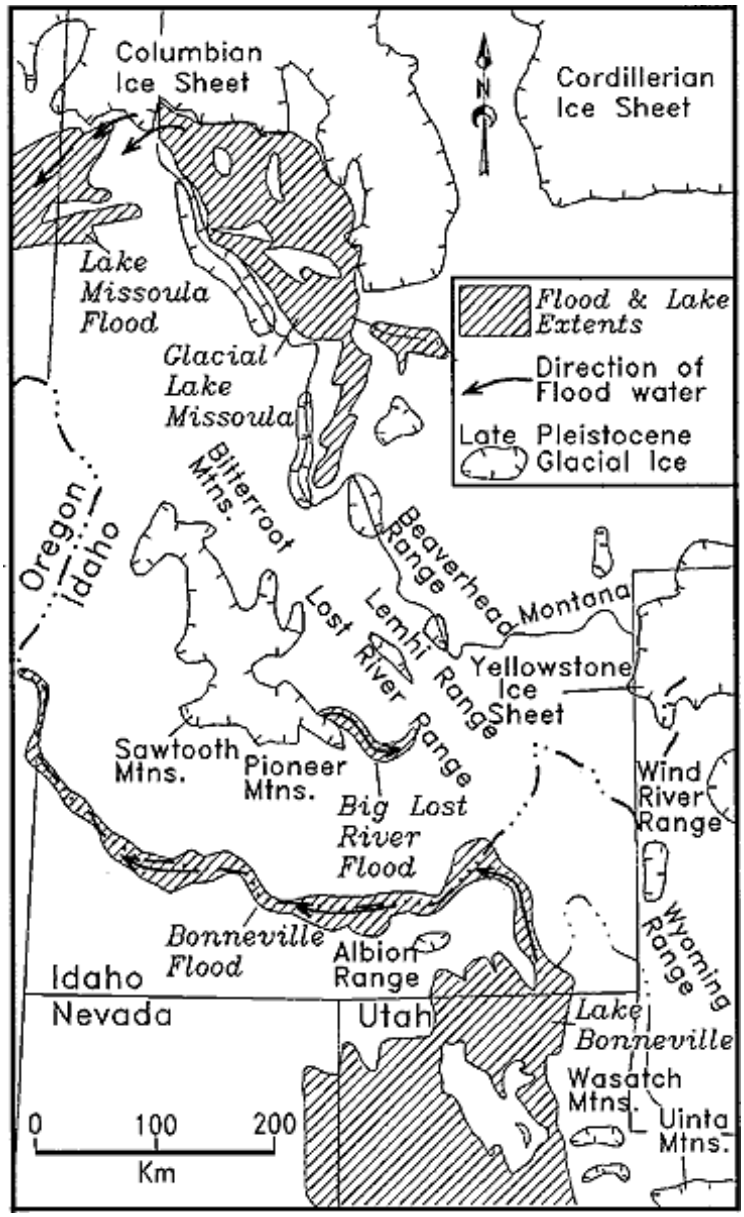

Figure 1. Simplified map showing areas of glaciation in Idaho, Montana, Utah and Wyoming, and glacial lakes Bonneville and Missoula (formed during deglaciation) and their subsequent flood paths. The Columbian and Cordilleran ice sheets in the northern portion of the map are lobes of the larger Laurentide ice sheet. From Link and Phoenix (1996).

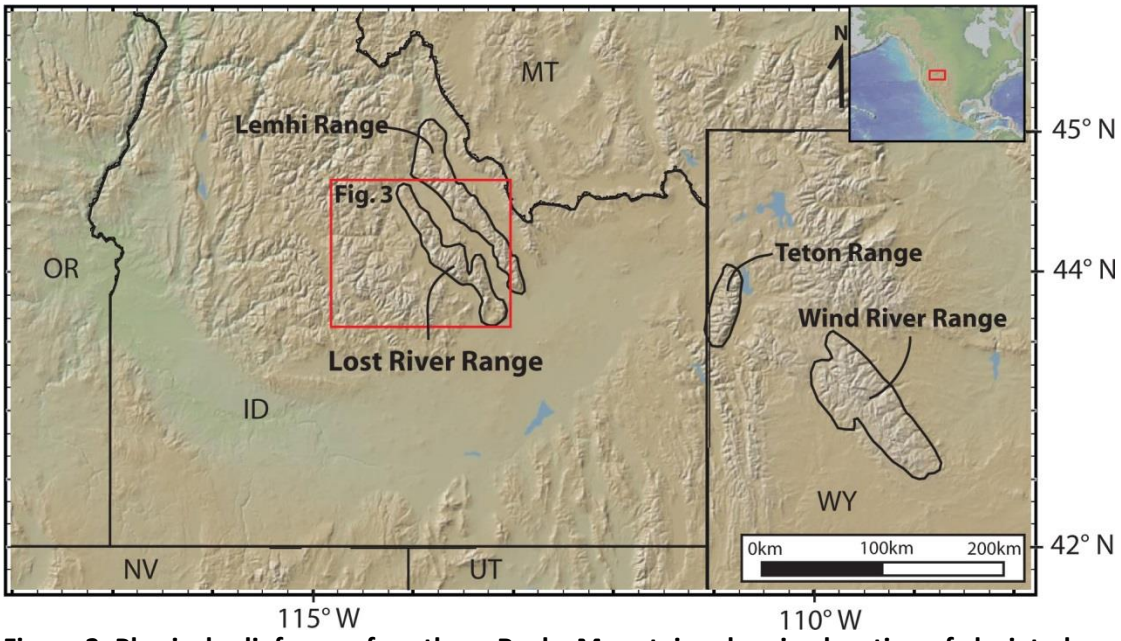

Figure 2. Physical relief map of northern Rocky Mountains showing location of glaciated or recently glaciated ranges mentioned in this report. Courtesy of GeoMapApp software.

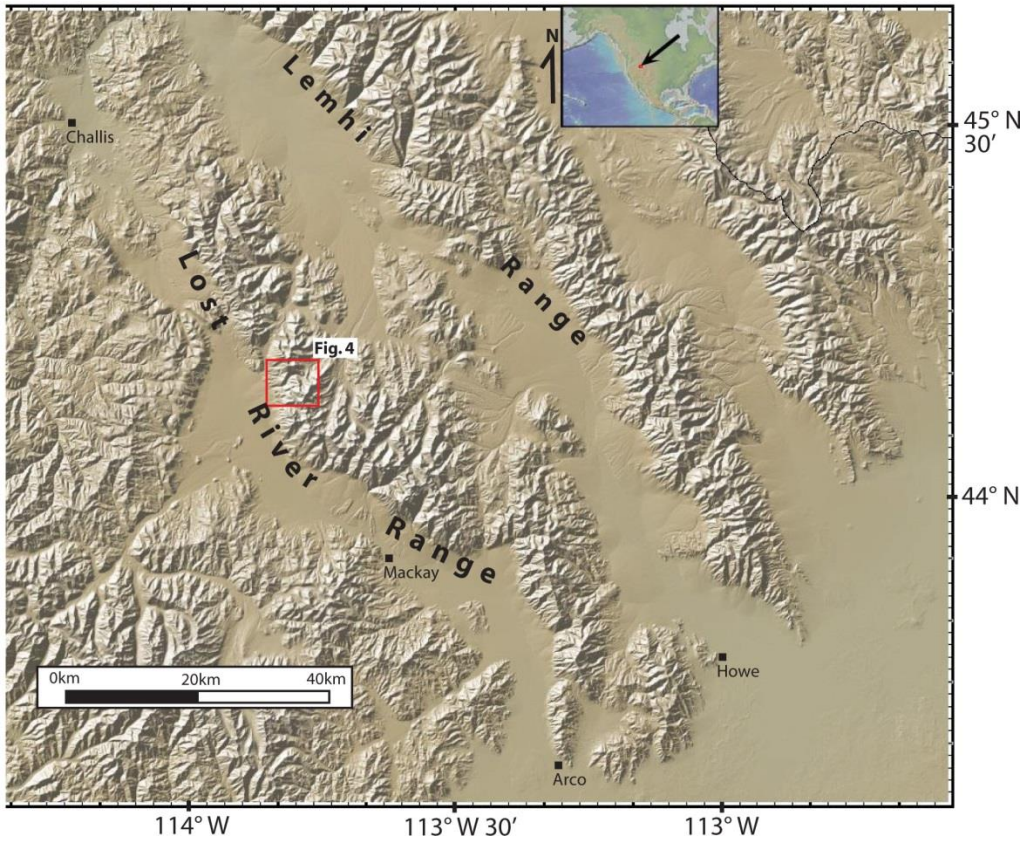

Figure 3. Physical relief map of east-central Idaho showing location of Lost River and Lemhi Ranges. Courtesy of GeoMapApp software.

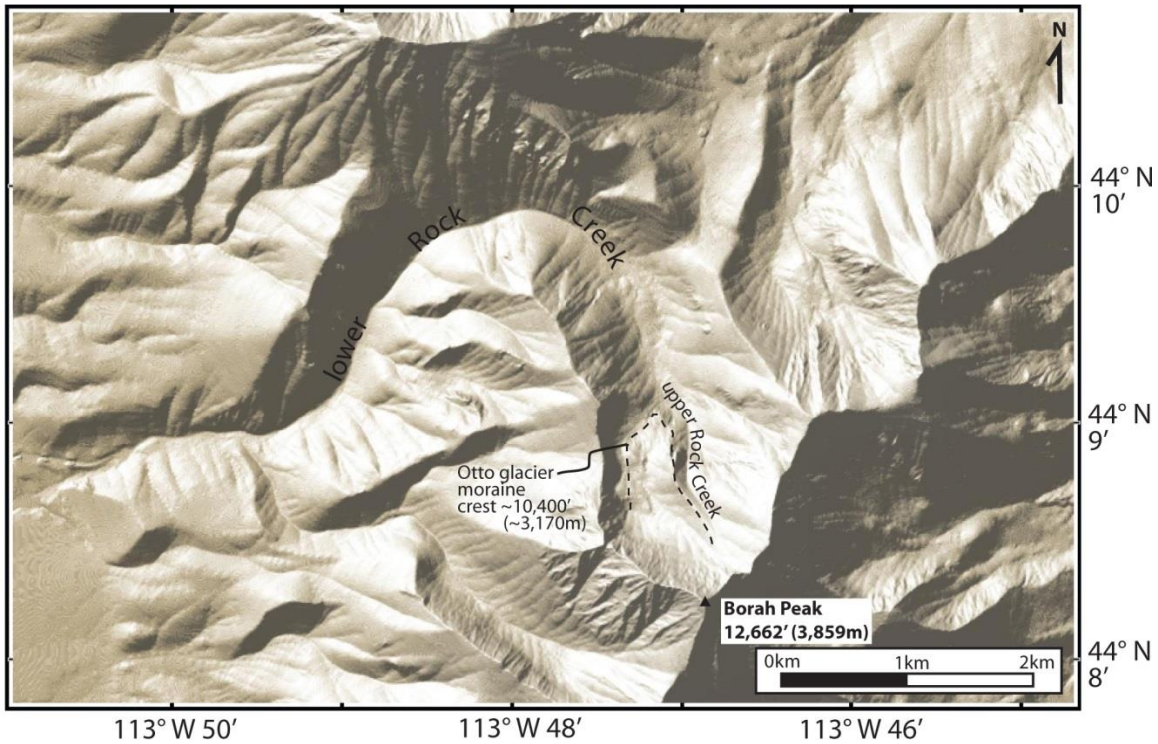

Figure 4. Physical relief map of Rock Creek and Borah Peak showing the crest of the recent or active moraine crest of the Otto Glacier. Courtesy of GeoMapApp software.

Discovery of the Otto Glacier

In 1974, the only recorded active alpine glacier in Idaho was discovered on the north face of Borah Peak at an elevation of about 3,170 meters (10,400 feet), in the Rock Creek drainage, just north-northeast of Mackay, Idaho (Otto, 1975) (Figs. 3 & 4). The initial investigation confirmed stratified ice exposed at the surface or beneath several centimeters to several meters of carbonate rock debris. The dimensions of the ice were found to be approximately 550 m (1,804 ft) in length and 250 m (824 ft) in width (including terminal moraine), an area of 137,500 m^2 (~0.05 mi sq). On the debris-free portion of the glacier, several open crevasses were observed, including the bergschrund crevasse, which separates the glacier from the bedrock headwall. On the debris-covered portion of the glacier, several debris-filled crevasses were observed.

Using 16 seismic depth soundings, Otto (1975) determined a maximum ice thickness of 64 meters (210 feet) near the middle of the glacier (Fig. 5). Three seismic transects of 4-6 stations each were taken at roughly one-third, one-half, and two-third portions of the rock-debris-covered part of the glacier. The furthest downstream depth sounding indicated an ice thickness of 15 m. The average ice thickness at the lower transect (approximately located one third of the distance upstream of the

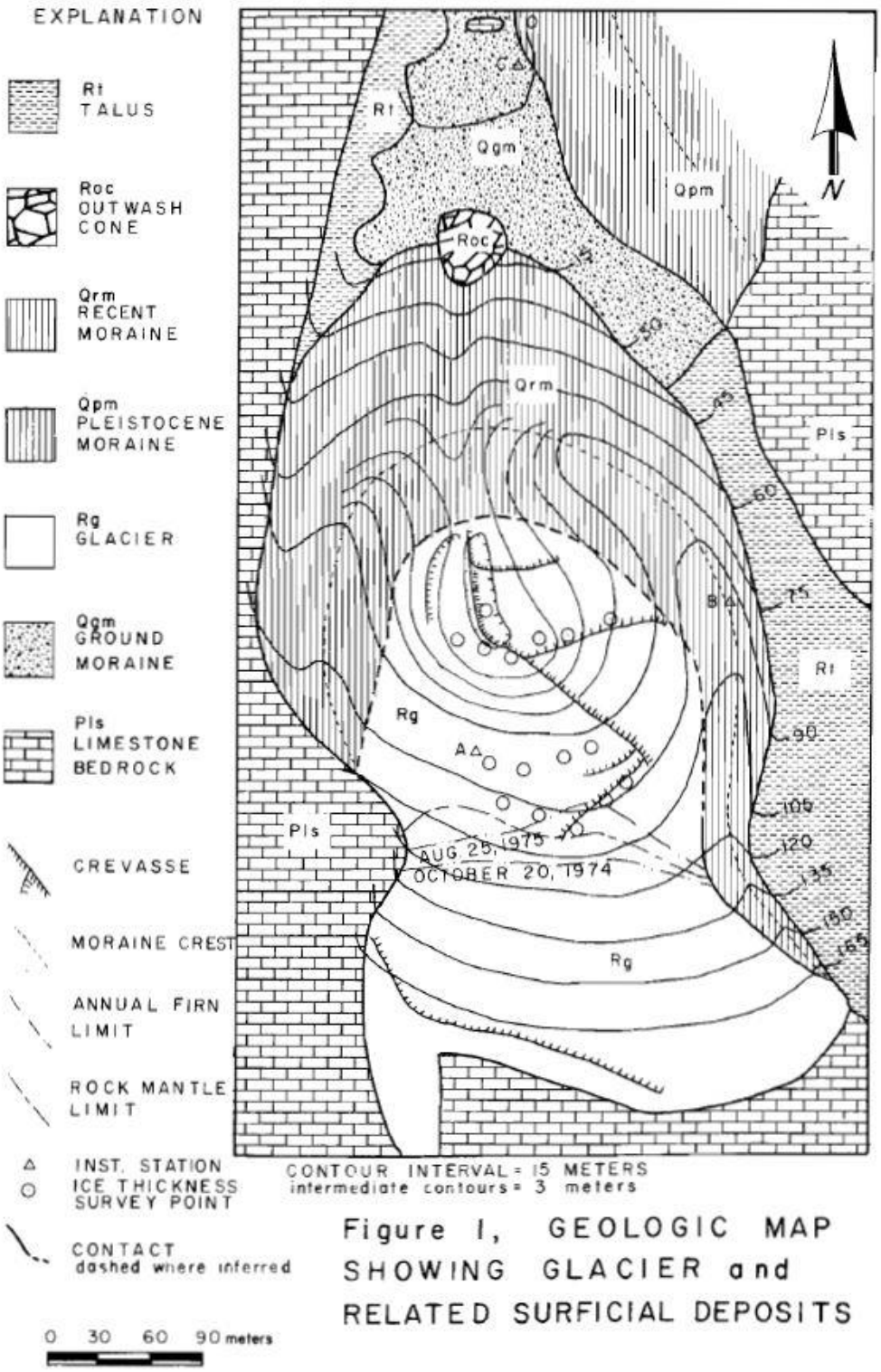

Figure 5. Geologic map of Rock Creek Cirque showing multiple moraines, seismic stations, 1974 and 1975 firn limits, crevasses, and elevation contours (see key). From Otto (1977).

glacier's toe) was 25 m. The average thickness at the glacier's midpoint was ~36 m, and the average thickness at the transect two-thirds upstream from the toe was 61 m. Preservation of the glacier was attributed to (1) its location, within the shadow of the north face of Borah Peak, (2) snow accumulation from sheet avalanches off the headwall and from a large nearby avalanche chute, and (3) further snow accumulation by drifting (Otto, 1975; 1977).

Monitoring continued over the ablation seasons of 1974 through 1976, during which it was determined the glacier had accumulated firn (granular snow) (Otto, 1977). During this monitoring period, several old crevasses had closed and several new ones had opened, signifying recent movement. The bergschrund crevasse extended 250 m along the headwall and was estimated to be 40-60 m deep (Otto, 1975). Within the Bergschrund, icicles were found to be rotated to various angles–evidence of movement (Fig. 6). A geologic map of Rock Creek Cirque (Fig. 5) shows the glacier, its recent to active moraine with an outwash cone (or outwash fan), and an older Pleistocene moraine further down the valley. Otto (1975) noted the outwash fan was at the downstream end of a gully cut into the moraine, and also noted a 5-cm-thick deposit of clay in the prominent depression on top of the glacier, just upslope of the gully (Fig. 5). Otto (1975) concluded that the clay was evidence of water ponding in the depression and the gully was evidence of flowing water. Informal monitoring of the glacier continued over the next 23 years (Otto, 2015, personal communication), with a detailed press release by Oakley (1986).

Figure 6: Bruce Otto is shown inside the bergschrund crevasse. To the right of Otto, icicles can be seen having been rotated clockwise.

At the foot of the meadow about 2 mi from the glacier lay an old moraine, a remnant of the past extent of the glacier. In the partial tree-covered valley, Dr. Monte Wilson, one of Otto's professors from Boise State University, took bore samples of trees and found ages around 500 years old, leading him to hypothesize that the glacier was no older than 500 years old (Oakley, 1986). Otto describes being able to feel the vibrations of the glacier. More recently, the Sloan family has picked up the torch in avidly

monitoring the glacier. They also describe being able to feel the glacier vibrate and hear pops and cracks within the ice that sound like “rice crispies” (Collin Sloan, personal communication, 2015). The most recent Sloan trip was a week before this study, on September 12, 2015. Altogether, the Otto glacier has been monitored over the last 41 years. Accounts from Otto himself and other investigators describe that the morphology has not changed much since its discovery.

2015 USFS METHODS

Upper Rock Creek was accessed by Mahogany Creek from the east. Traditional mountaineering equipment was used to gain access to the glacier and safely enter one crevasse (e.g., hard hat, crampons, ice axe, gloves, etc.). Survey equipment tied to a precise GPS point was located roughly 1,130 meters (0.7 miles) away from Rock Creek Cirque. A test shot between the surveyor and the Mahogany Creek parking area as well as a back-sight was used to calibrate the survey. The surveyor then sighted to the technician along the crest of the Otto glacier moraine and the tips of the 30-foot-deep crevasse, (herein called Crev-1). Survey point error is within one meter. The more accurate survey points were used to correct Google Earth elevation, which were determined to have errors of up to 9 meters (30 feet).

Aerial imagery, topographic maps and historic Google Earth imagery were used to map the surface distribution of present crevasses and to construct a cross section of the glacier. Area estimates were made in GIS using confirmed GPS locations of stratified ice in conjunction with National Agriculture Imagery Program (NAIP) imagery.

Ice sample were taken from the most pristine ice available with an ice axe or rock hammer. Locations where recent frozen runoff may have contaminated the ice, such as fresh icicles or snow banks, were avoided. Only locations where stratified ice was confirmed were chosen and ice was sampled within several inches of the surface. However, contamination is possible given that the sampled ice was exposed to atmospheric conditions including direct precipitation such as fog or rain, which may have frozen to the ice surface.

The samples were kept frozen in ziplock bags until shipment, when they were allowed to melt. Once melted, the water was transferred to opaque plastic bottles with no evaporative headspace. Similarly, the original water sample, 5BG15, was taken by completely submerging the opaque plastic bottle so as to remove all air before tightening the lid.

The analyses were done at the CAMAS facility at Idaho State University. Samples were analyzed using Thermo Scientific, High Temperature Conversion Elemental Analyzer (TC-EA) interfaced to a Delta

V advantage mass spectrometer through the ConFlo IV system. Using SGE autosampler syringes, 0.5 microliter of water is injected into the hot glassy carbon tube held at 1400◦C where the water is pyrolyzed to generate hydrogen and carbon monoxide gases. The gases generated are carried in a helium stream into a GC column at 85◦C to get separated before being diluted in the ConFlo IV and passed to the mass spectrometer for analysis. Six standards were run with the samples, two (USGS RSIL: W-67400 and USGS RSIL: W64444) were used to normalize the data where as LGR1A, LGR2A, LGR3A and LGR4A were analyzed as unknowns to monitor the accuracy of the data.

RESULTS

The 2015 USFS expedition to Rock Creek took place on September 24, 2015. Several inches of snow had fallen a week prior, but over the course of a warm week, snow cover had diminished. Locations of the moraine crest, bergschrund crevasse, a smaller open crevasse just below the bergschrund, and debris-mantled crevasses were identified. The survey team measured points along the crest of the moraine, and a smaller open crevasse, here called Crev-1 (Figs. 7 & 8), was entered and explored. Bedrock was seen along the northern wall of the bergschrund crevasse, which was determined too unsafe to enter (Fig. 9).

Crev-1 was found to be at least 12 meters (~40 feet) deep, with an ~2 meter-deep (~6.5 feet) firn depth followed by 9 meters (30 feet) of dense stratified ice (Fig. 10). At the bottom was a frozen meltwater pond (Fig. 10). Neither bedrock nor rock debris were found at the bottom. Two ice samples were taken from Crev-1 for isotopic analysis. Sample 1BG15 was taken from dense stratified blue ice about 6 meters (20 feet) below the firn line (Fig. 10), and sample 2BG15 was taken 9 meters below the firn line at the bottom of the crevasse (Fig. 11). Within the second room in Crev-1, ice stalactite features as well as a closed tilted ceiling indicated possible rotation (Figs. 12 & 13). Both “paleo-icicles” and formerly vertical walls of the sealed crevasse ceiling appear to be tilted the same amount in the same direction.

Using the survey data in conjunction with Google Earth elevation data and the ice thicknesses from Otto (1975) (Fig. 14), a longitudinal cross section of the glacier was constructed along its centerline (Fig. 15). Use of the ~40-year-old seismic data from Otto (1975) is still relevant because the glacier size and morphology has not changed significantly over the years (Otto, personal communication, 2015). This is supported by 2015 data which shows the elevation change between the bedrock floor of Rock Creek Cirque (~10,200 feet) and the elevation of the moraine (10,400 feet) has not changed, suggesting the ice thickness has not decreased since the original survey.

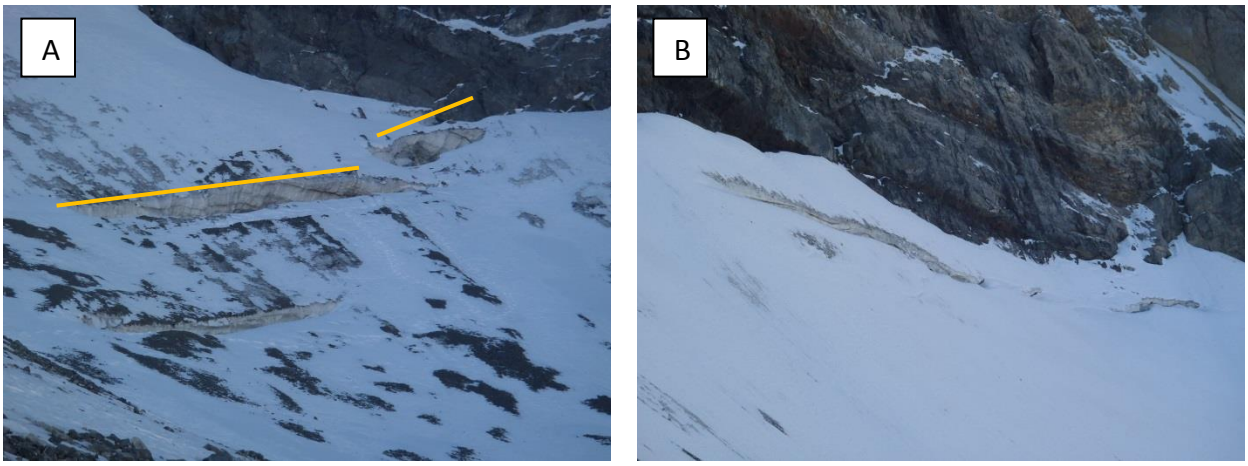

Figure 7. A: 2015 Photo of the bergschrund crevasse (higher) and the lower smaller crevasse, Crev-1, taken from the eastern moraine crest. Compare the en echelon (stepwise) crevasse pattern (accentuated by orange lines) to the same pattern in Figure 8B: Zoomed photo of western continuation of bergschrund crevasse.

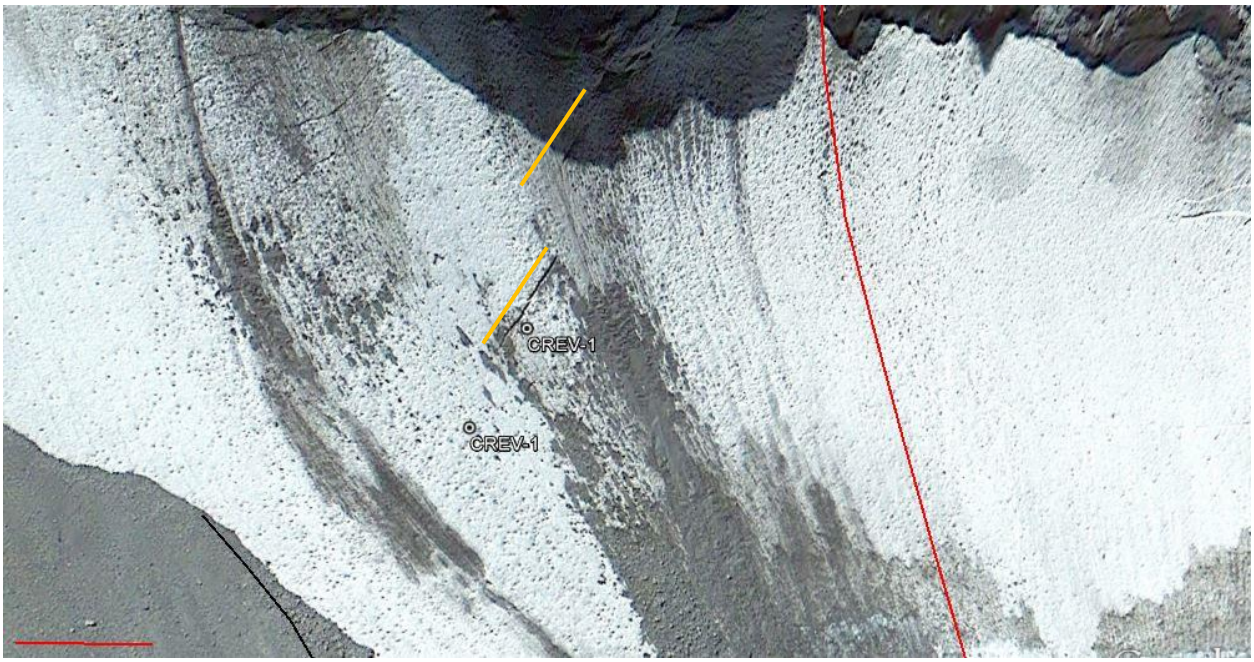

Figure 8. Close up of Crev-1 points surveyed in September 2015 overlaid onto 2013 Google Earth image. Comparing Figure 8 to Figure 7, the stepwise crevasse in the Figure 8 image is likely the en echelon fracture pattern of the incipient opening of the bergschrund seen in the 2015 photo (Fig. 7). Red scale bar in lower left is 20 m.

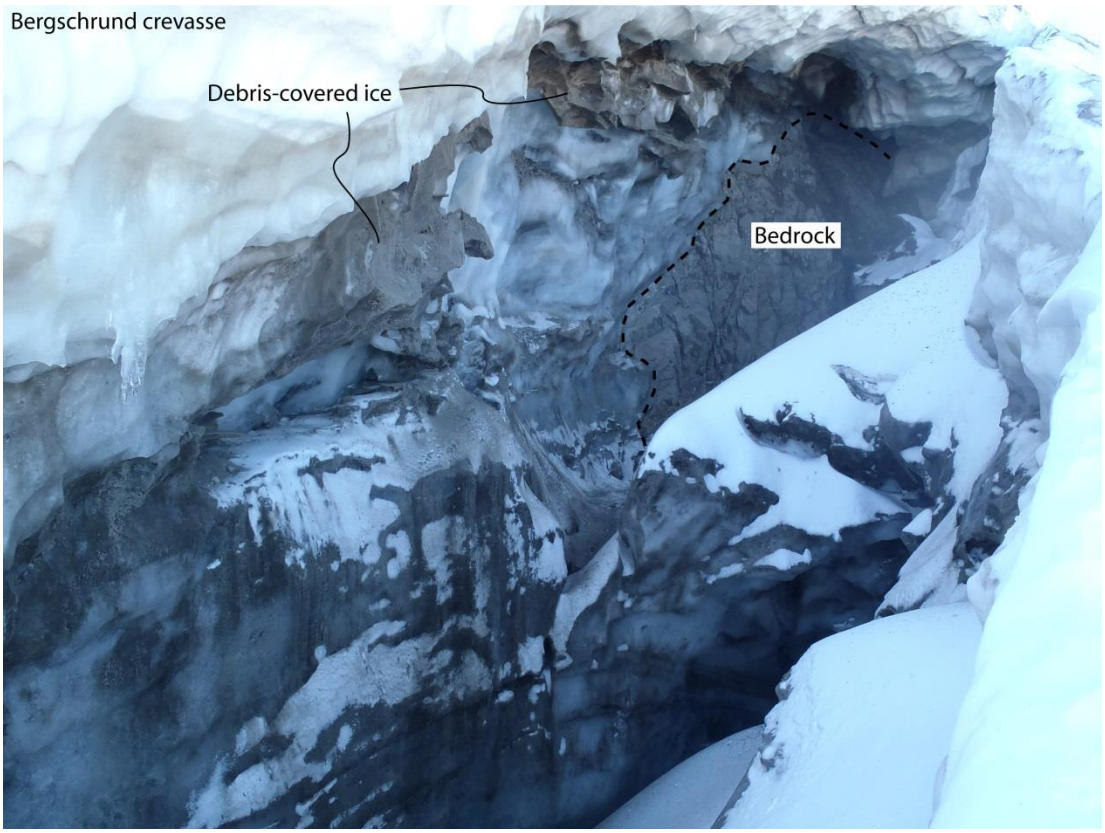

Figure 9. 2015 photo of the bergschrund crevasse showing bedrock and debris-covered or dirty ice.

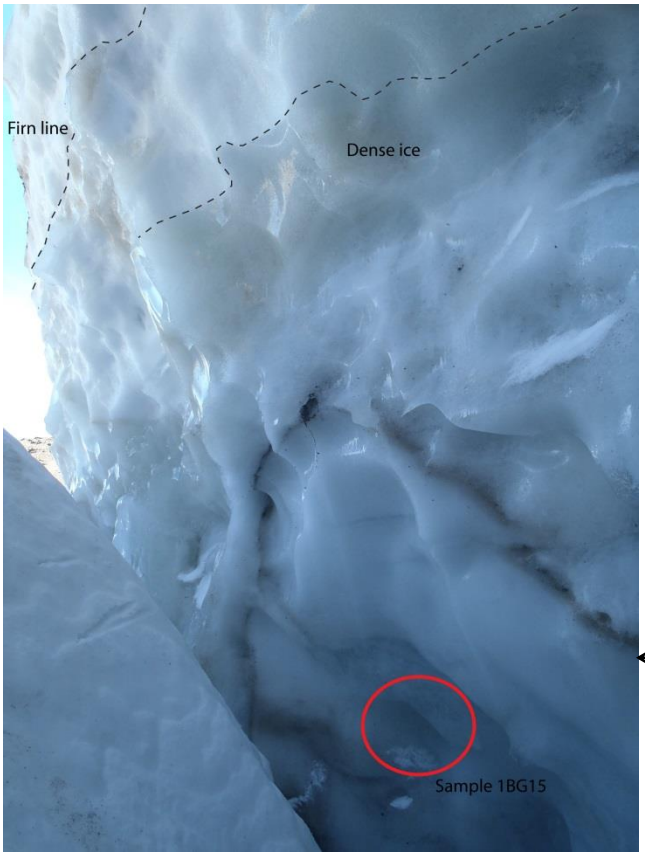

Figure 11: 2015 Photo inside first room of Crev-1, showing frozen meltwater floor. Location of isotopic sample (2BG15) shown by red circle.

Figure 10: 2015 Photo inside first room of Crev-1, showing firn line (upper dashed line) and lower dashed line marking stratified blue ice. Location of isotopic sample (1BG15) shown by red circle.

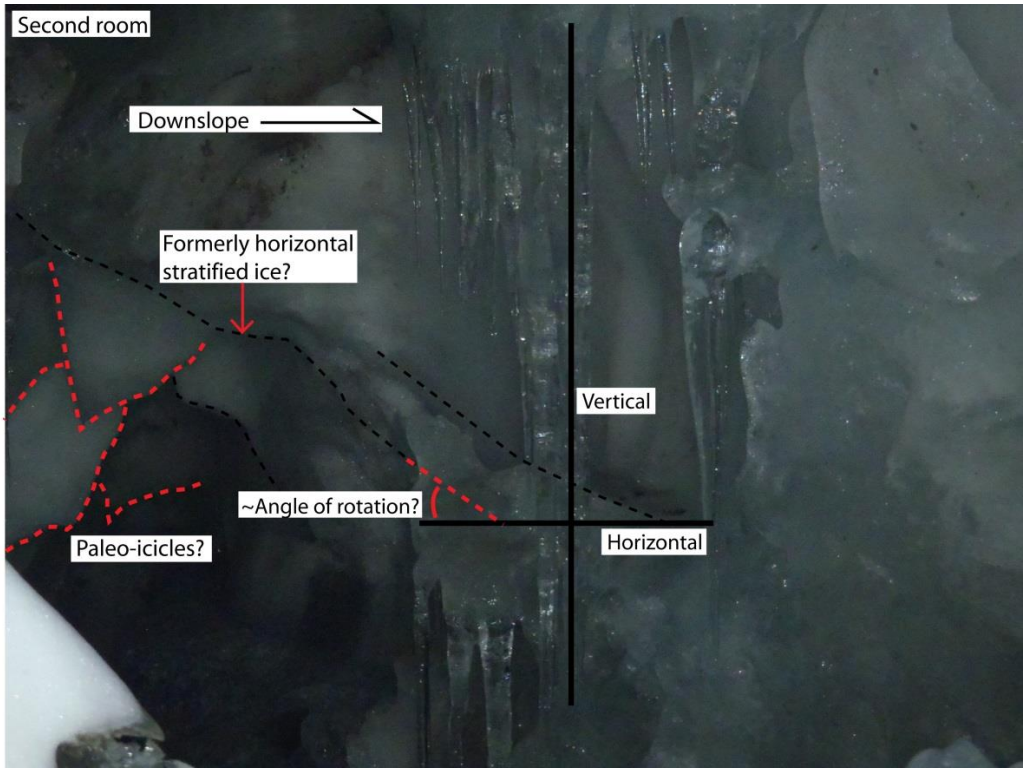

Figure 12. 2015 Photo inside second room of Crev-1, showing ice stalactite structures that may be "paleo-icicles" that have rotated clockwise relative to the fresh vertical icicles also in photo.

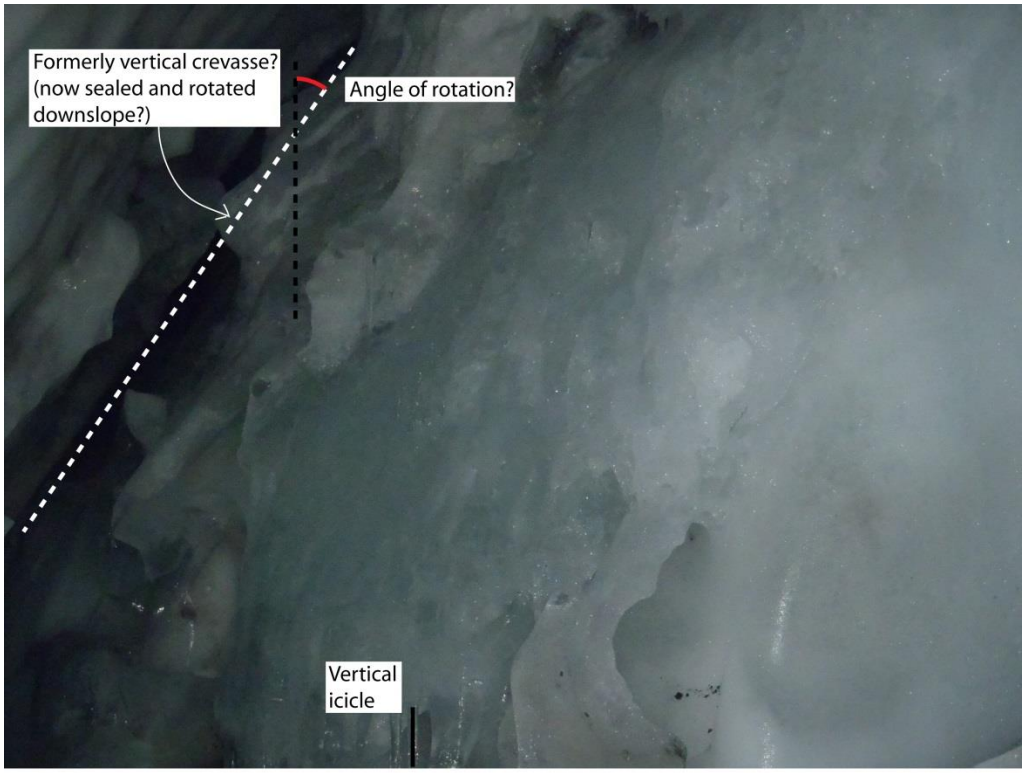

Figure 13. 2015 Photo inside second room of Crev-1, showing the closed crevasse ceiling that is tilted clockwise in the downstream direction. Note fresh vertical icicles also in photo.

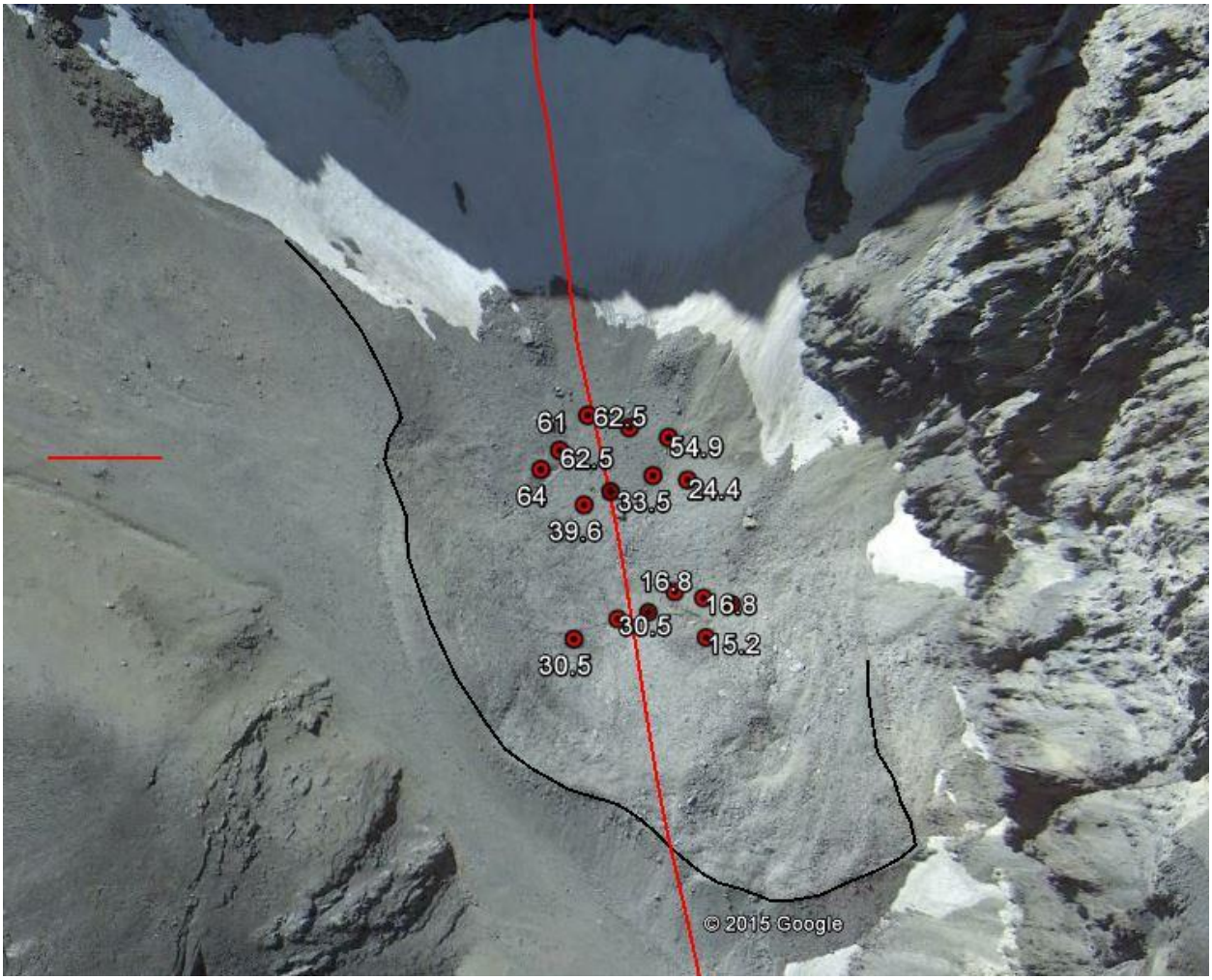

Figure 14. Seismic survey stations from Otto (1975) in relation to red longitudinal section (full extent not shown) showing ice thicknesses measured at each station. Moraine crest outlined in black. Red scale bar is 50 m.

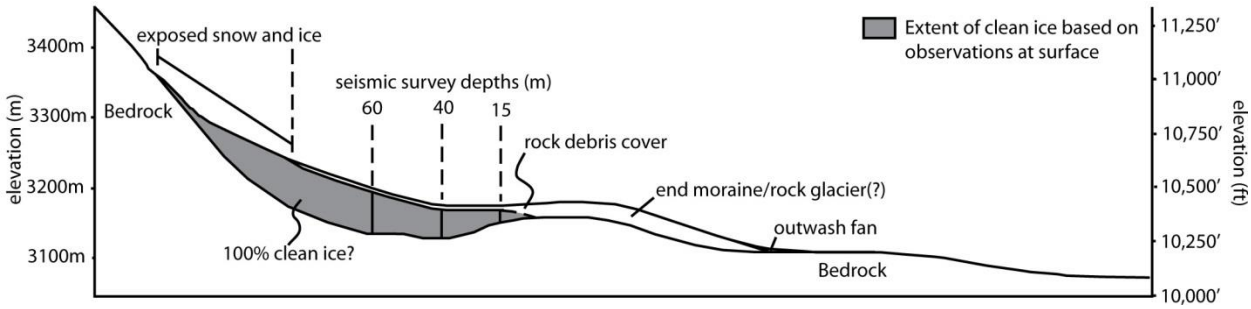

Figure 15. Longitudinal cross section of the Otto glacier in Rock Creek Cirque showing seismic survey depths, extent of ice exposures and ice thickness. No vertical exaggeration

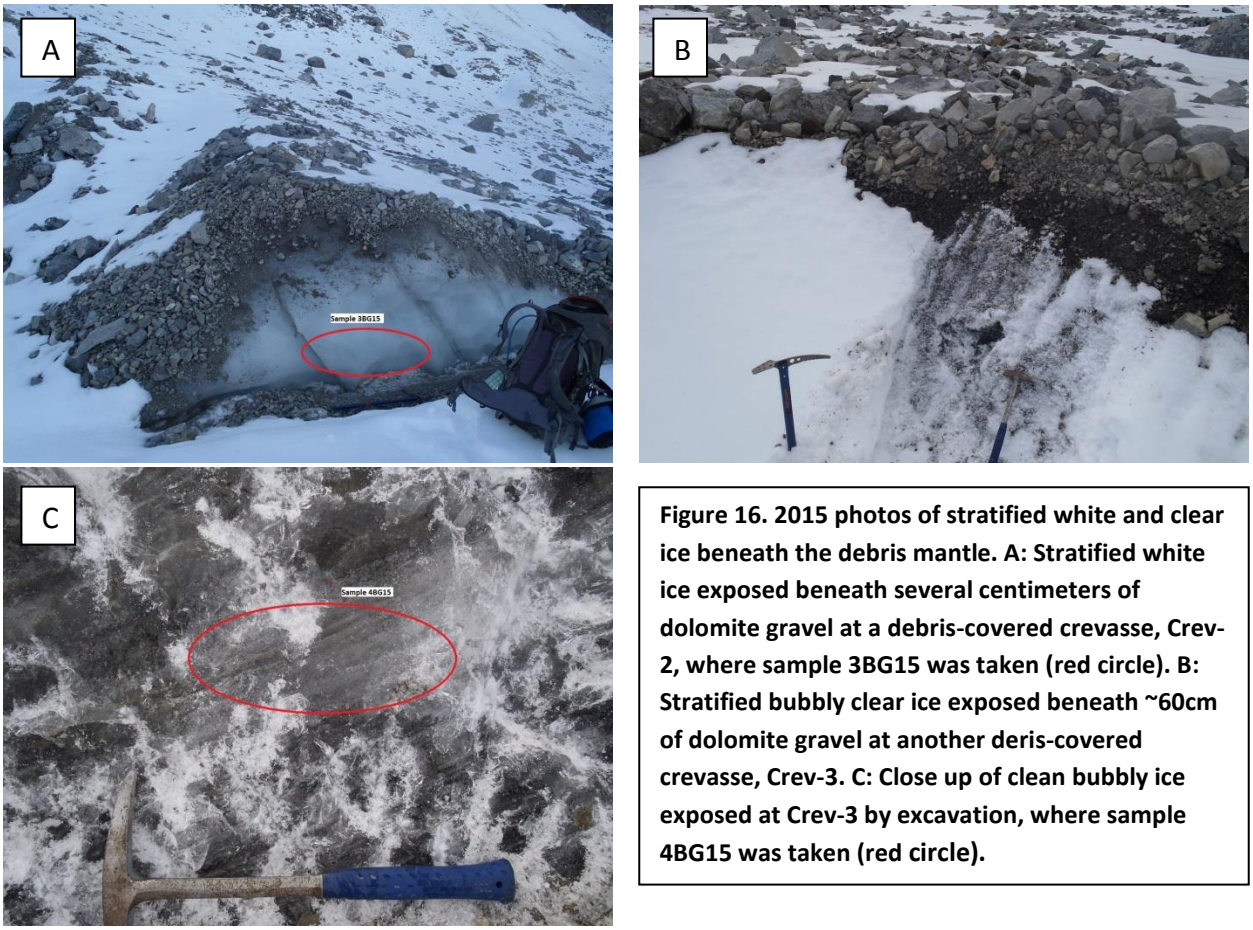

Figure 16. 2015 photos of stratified white and clear ice beneath the debris mantle. A: Stratified white ice exposed beneath several centimeters of dolomite gravel at a debris-covered crevasse, Crev-2, where sample 3BG15 was taken (red circle). B: Stratified bubbly clear ice exposed beneath ~60cm of dolomite gravel at another deris-covered crevasse, Crev-3. C: Close up of clean bubbly ice exposed at Crev-3 by excavation, where sample 4BG15 was taken (red circle).

Stratified ice, free of interstitial debris, was confirmed at the surface at multiple locations on the debris-covered portion of the glacier (Fig. 16). Observed ice locations were used to create the estimated clean ice portion of the glaicer (shaded area on Figure 15). Figure 15 shows about two-thirds of the clean ice portion of the glacier is covered by rock debris, with the thickest part of the glacier (64 m) occurring over the length of the middle third. Otherwise, the mean thickness of upper and lower thirds of the glacier appears to be between 40-50 m. The portion of the glacier making up the terminal moraine may have an ice core and thus might be a rock glacier.

Velocity Estimates

An attempt was made to detect surface movement of the glacier using the historic Google Earth photos that date back to 1992. Although crevasses and large rocks are detectible throughout the 1992 to 2009 imagery, they were determined too low in resolution and too high in photo rectification error in

various directions (up to 3 m or more) to use. Imagery from 2011, 2013 and 2014 are fairly accurate with imagery from 2013 and 2014 being of high-resolution. First, image error correction was attempted between 2011 and 2013 images and between 2013 and 2014 images by measuring changes in distance of stable bedrock polygons (Fig. 17). This step was performed on stable bedrock features in all cardinal directions of the glacier, all of which obtained similar results. Next, features on the glacier were traced over the 2011, 2013 and 2014 imagery and compared to stable bedrock to detect any possible movement. The first feature traced was a large rock known as "Lunch Rock" along with nearby crevasses (Fig. 18). The results show between 100-150cm of image error between 2011 and 2013, and 50cm of error between 2013 and 2014 (both toward the NW). Total movement of Lunch Rock and nearby crevasses from 2011 to 2013 was 250-300cm, and 120-190cm between 2013 and 2014 (toward the NNW, or *down*-slope). Correcting for true *down*-slope movement (subtracting the image error from total observed) shows an additional *down*-slope movement of 50-140cm per year (Table 1).

Using this method for rocks on and off the glacier yields the same results as when comparing the stable bedrock to Lunch Rock. Further upslope on the glacier, three rocks (listed in Table 1 as "Rock-1") and the debris-covered crevasse, Crev-2, were traced in 2011, 2013 and 2014 Google Earth images (Fig. 19). The apparent distance that the three traced rocks at Rock-1moved were within 10 cm of each other, so were averaged and reported only once. The results show that image error accounts for a total of 65-280 cm of apparent movement between each image, but that an additional 85-160cm of movement is detected per year (Table 1). The average velocity of all measured features ranges from ~72 to 163cm/year.

Taking a different approach, a theoretical strain rate (or velocity) of the glacier was calculated to determine what speed would be theoretically possible given the known variables of thickness, slope, ice thickness, and gravitational force. Using several simplifying assumptions, the Glen-Nye flow law (Glen, 1952; Nye, 1952) relates stress and strain and models internal deformation in glacial ice. The equation for a half-cylinder shaped glacier is as follows:

$$\textit{Equation 1: } \varepsilon = 1/2k\tau^n$$

Where ε is strain rate, τ is stress, n is a constant between 2-4 that increases with lower temperature, and k is another temperature-dependent constant. Stress (τ) is the product of gravity (9.8 m/s^2), ice density (917 kg/m^3), and SIN of the slope. A value of 1.17 was used for k. For most alpine glaciers, n is equal to 3, but because the Lost River Range experiences mean monthly temperatures ranging from 25-90 °F, n values of 2 and 3 were used and reported in

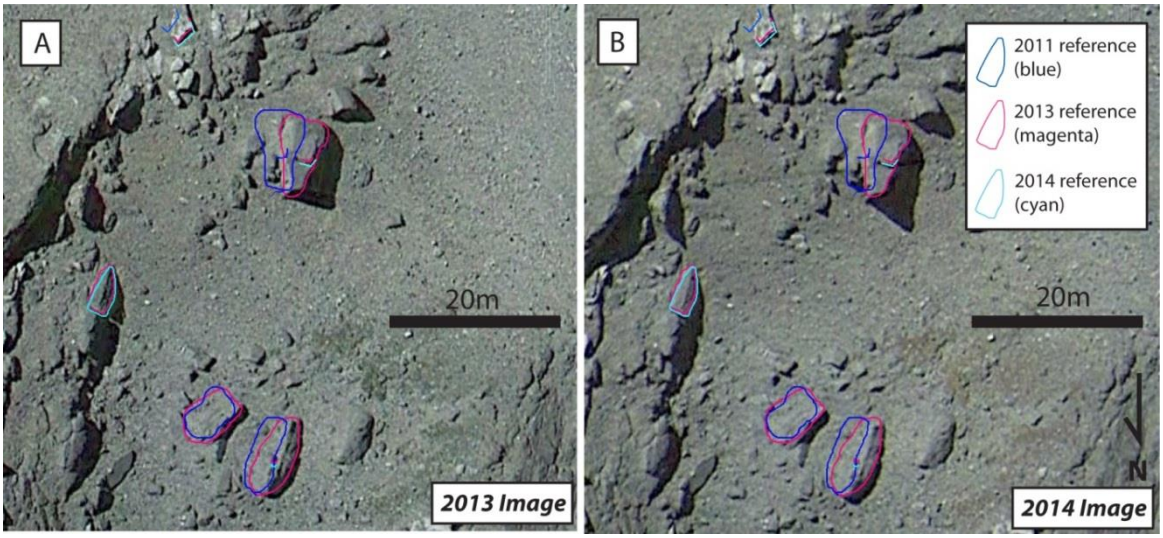

Figure 17. Image error detection using traced polygons of known bedrock outcrops from 2011, 2013 and 2014 Google Earth imagery (poorly resolved 2011 imagery not shown). A: 2013 image showing error between 2011 (blue), 2013 (magenta), and 2014 (cyan) images. B: 2014 image with same overlaid lines as in Fig. 17A, showing an almost imperceptible ~50cm error between 2013 and 2014 images.

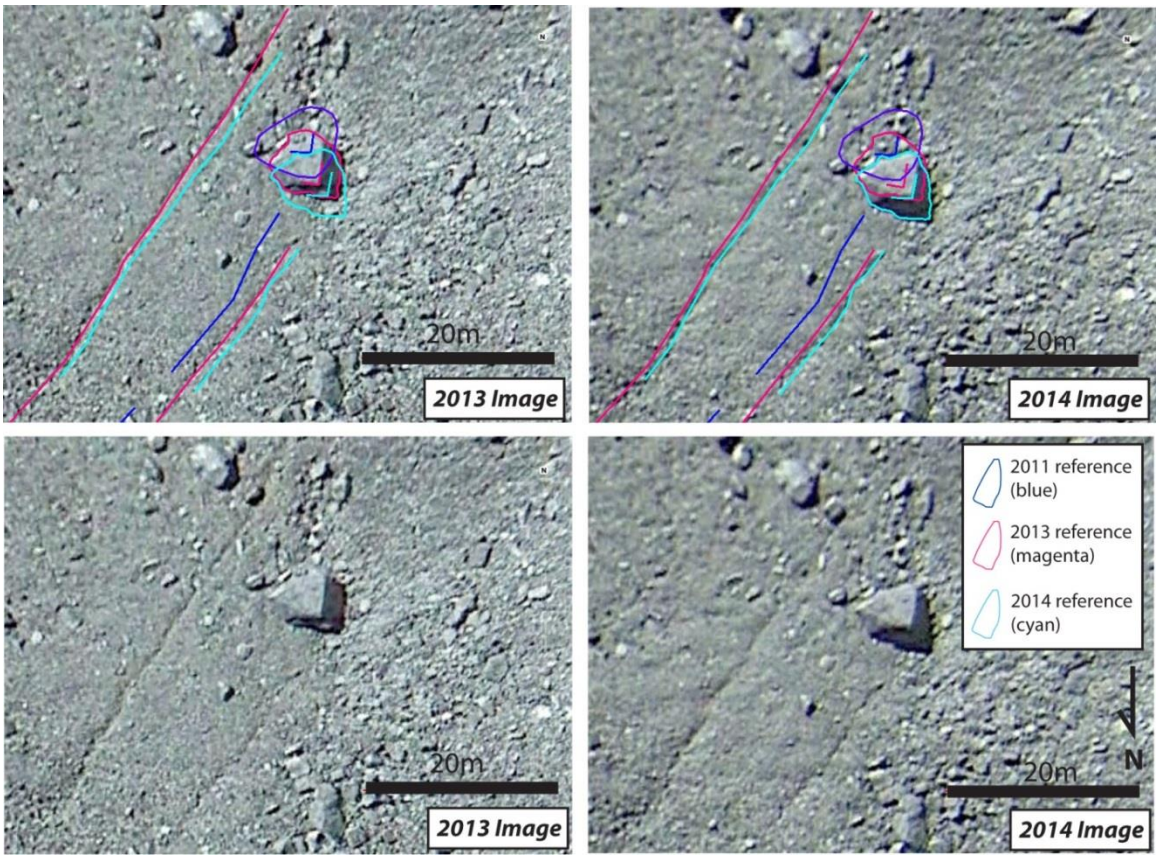

Figure 18. 2013 and 2014 Google Earth images showing the total image error plus extra surface movement between 2011 (blue), 2013 (magenta), and 2014 (cyan). Unlabeled photos below for comparison.

Table 1. Surface movement calculations using Google Earth imagery between 2011 through 2014*

Feature	Google Earth image years observed	Min Measured displacement (cm)	Max Measured displacement (cm)	Min Image Correction (cm)	Max Image Correction (cm)	Min Lunch Rock movement per year (CM)	Max Lunch Rock movement per year (CM)
Lunch Rock	2011-2013	250	300	100	150	50	100
Lunch Rock	2013-2014	120	190	50	50	70	140
Lunch Rock	2011-2014	370	490	150	200	57	113
Rock-1	2011-2013	370	470	150	200	85	160
Rock-1	2013-2014	180	200	65	80	100	135
Rock-1	2011-2014	550	670	215	280	90	152
Crev-2	2011-2013	215	360	150	200	8	105
Crev-2	2013-2014	220	280	65	80	140	215
Crev-2	2011-2014	435	640	215	280	52	142
Average (2011-2014)						72	140
Std. Dev. (2011-2014)						+/- 37	+/- 35
Average (2013-2014)						103	163
Std. Dev. (2013-2014)						+/- 35	+/- 48

*See Figures 17-19 for imagery

Tables 2 and 3, respectively. Tables 2 and 3 show the calculated theoretical glacier velocities from several points along the glacier where its thickness is known.

Rearranging and modifying the Glen-Nye Flow law to solve for ice velocity of a glacier with a half-cylinder shape using different constants we obtain:

$$\textit{Equation 2: } U_s = A/4*(1/2\rho S)^n*H^4$$

Where U_s is the surface velocity, A and n are temperature-dependent constants, ρ is the density of ice, S is the surface slope, and H is the ice thickness (Bob Anderson, personal communication, 2015). Values for A, 6.7E-17 and 2.2E-16, were suggested as mid-range values that could be used knowing that (1) the equation is already greatly simplified, and (2) the true temperature of the glacier is needed to use the equation the way it was intended (Bob Anderson, personal communication, 2015). The velocity results presented in Table 4 use the same parameters and locations as in Tables 2 and 3.

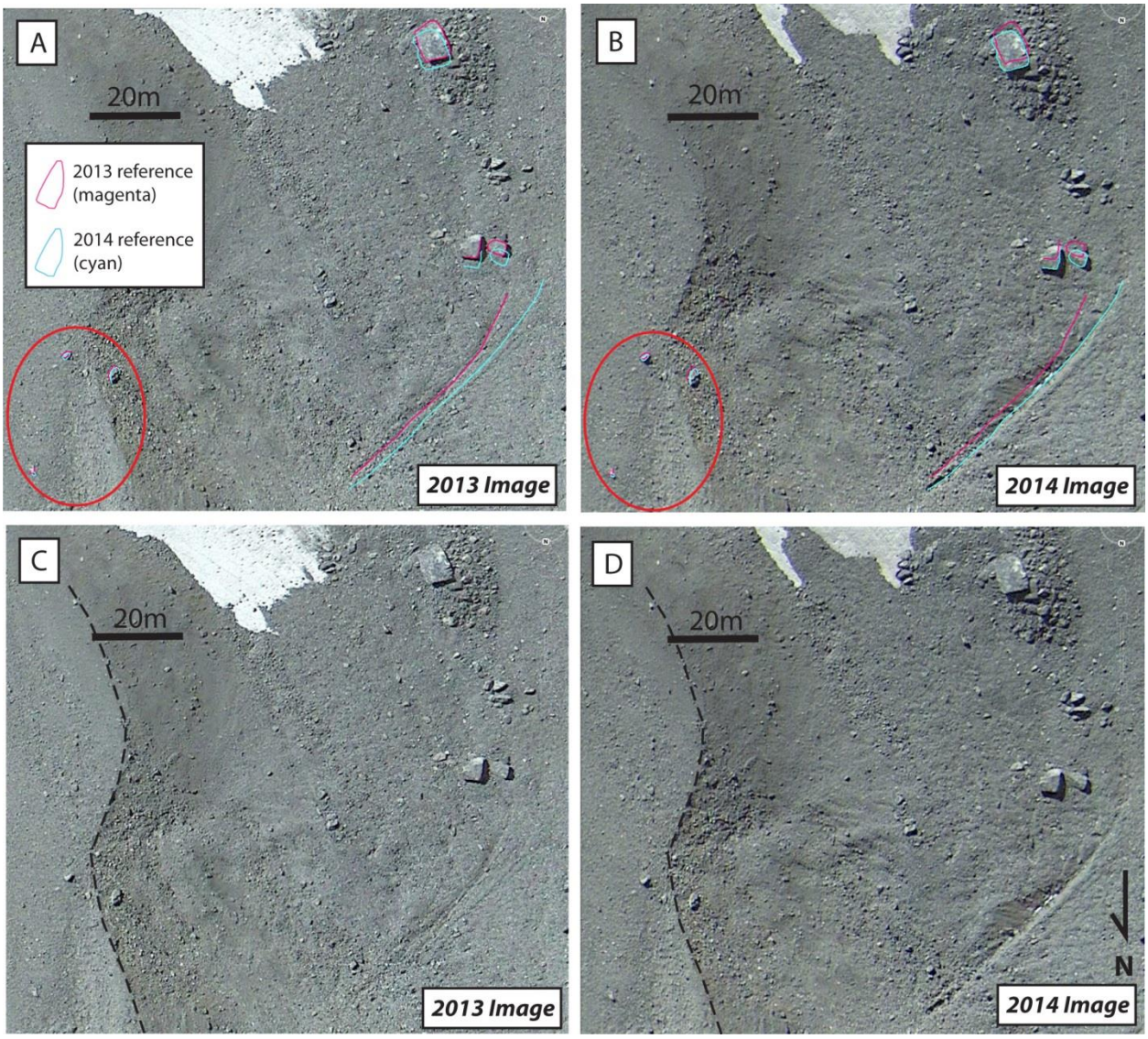

Figure 19. A and B: 2013 and 2014 Google Earth images of "Rock-1" and "Crev-2" locations. Rock-1 informally refers to the 3 traced rocks on the right side of the figure. The figure shows the total image error plus extra surface movement between 2013 (magenta), and 2014 (cyan). Note the stable rocks off-glacier circled in the lower left. Calculations for 2011 movements were made but are not shown (Table 1). C and D: Unlabeled photos below for comparison showing the location of the moraine crest (dashed black line).

Table 2. Stain rate calculations using $\varepsilon = k\tau^n$*

Feature	thickness (m)	slope	SIN(slope)	stress (bars)	strain rate (cm/yr)
Crev-1&2	60	0.6	0.56	1.52	564.97
Glacier Midpoint	40	0.5	0.48	0.86	102.47
Lunch Rock	35.8	0.4	0.39	0.63	39.37
Glacier toe	15	0.09	0.09	0.06	0.04

*where constants k = 1.17, and n = 3

Table 3. Stain rate calculations using $\varepsilon = k\tau^n$*

Feature	thickness (m)	slope	SIN(slope)	stress (bars)	strain rate (cm/yr)
Crev-1&2	60	0.6	0.56	1.52	317.21
Glacier Midpoint	40	0.5	0.48	0.86	101.64
Lunch Rock	35.8	0.4	0.39	0.63	53.72
Glacier toe	15	0.09	0.09	0.06	0.50

*where constants k = 1.17, and n = 2

Table 4. Stain rate calculations using $U = A/4*(0.5[\rho gh]^n)*H^4$*

Feature	thickness (m)	slope	SIN(slope)	stress (bars)	*A* value	Velocity (cm/yr)
Crev-2 (min)	60	0.6	0.56	1.52	6.7E-17	701.54
Crev-2 (max)	60	0.6	0.56	1.52	2.2E-16	2303.56
Lunch Rock (min)	35.8	0.4	0.39	0.63	6.7E-17	58.26
Lunch Rock (max)	35.8	0.4	0.39	0.63	2.2E-16	191.29
Glacier toe (min)	15	0.09	0.09	0.06	6.7E-17	2.74
Glacier toe (max)	15	0.09	0.09	0.06	2.2E-16	9.00

*where constants A = 6.7E-17 and 2.2E-16 for min and max calculations, respectively
*n = 3

The theoretical strain rates and velocities vary greatly depending on what temperature-dependent constants are used. Additionally, the two equations produce different results due to the different sets of assumptions and constants used. Therefore, we can only use these data for preliminary, first-order interpretations.

Comparison between the strain rate, velocity results, and the surface movement data shows considerable overlap. Theoretical rates at Lunch Rock (40-200 cm/yr) match very well with what is observed (50-140 cm/yr). The strain rate and velocity estimates at the toe of the glacier indicate that little to no ice movement is possible under these parameters, supporting the notion that the terminal moraine has not been observed to move over the last 41 years. However, the calculated rates at Crev-2 range between 3m/yr to 23 m/yr, much greater that what is observed (8-215 cm/yr). Several potential sources of error could have led to the discrepancy. Perhaps the elevation error associated with Google Earth images, found to increase with increasing topography, led to an overestimation of slope. Also, the constants used may be incorrect for the conditions on this glacier. Perhaps unseen factors such as unseen rock debris frozen between ice layers has increased friction or slowed down the internal strain rate. Further work is needed to answer these questions.

δ2H and δ18O Isotope Introduction

Delta deuterium (δ^2H, or D) and delta-O-18 ($\delta^{18}O$) data are helpful in interpreting the hydrologic cycle of the precipitation (rain and snow) that have been deposited and accumulated to form the ice making up the glacier and also the precipitation that has potentially modified the ice. The $\delta^{18}O$ value is a ratio between isotopes ^{18}O and ^{16}O:

$$\delta^{18}O = \left(\frac{\left(\frac{^{18}O}{^{16}O}\right)_{sample}}{\left(\frac{^{18}O}{^{16}O}\right)_{standard}} - 1 \right) * 1000\ ‰$$

Delta deuterium is obtained a similar way using the ratio between ^2H and ^1H. Both δ^2H and $\delta^{18}O$ record precipitation events and evolve toward lighter and more negative values after each successive event.

As a body of water with a standard base isotopic value (e.g., Global Mean Water Line, or GMWL) evaporates, the lighter oxygen isotope (^{16}O) is preferentially taken up into the atmosphere in the vapor phase. As the body of air cools, water condensates, and the heavier oxygen isotope (^{18}O) is preferentially drawn out into the water phase. This isotopic fractionation operates with each successive precipitation event, therefore evolving the isotopic value lighter, or more negative values. Due to the simple relationships that air is cooled when it rises and precipitation results from a decrease in temperature, both δ^2H and $\delta^{18}O$ decrease with both latitude and elevation (Clark and Fritz, 1997). Very negative δ^2H and $\delta^{18}O$ values can therefore serve as a proxy for higher latitudes, higher elevations, and colder temperatures. In the case of very thick glacial ice deposited at Earth's poles, this process occurred unceasingly over hundreds of thousands of years during the Pleistocene. The result was a ^{16}O-enriched or (lighter $\delta^{18}O$) ice cap and a ^{18}O-enriched ocean (heavier $\delta^{18}O$). In this example the $\delta^{18}O$ value can serve as an age proxy, with more negative values representing older ice or meltwater. However, whereas these relationships operate well in closed systems and in polar settings, post-depositional processes may modify the isotopic composition of glacial ice in more dynamic and temperate settings.

2015 δ2H and δ18O Isotope Data

In order to best characterize the hydrologic cycle of and around the Otto glacier, isotopic ratios (δ^2H and $\delta^{18}O$) were obtained from four ice samples and one meltwater sample taken from a small pond at the downstream end of upper Rock Creek. Sample 1BG15 was taken from a 20 foot depth inside Crev-1 (Fig. 10). Sample 2BG15 was taken from a 30 foot depth at the floor of Crev-1 (Fig. 11). Sample 3BG15

was taken from the debris-covered Crev-2 (Fig. 16A) and sample 4BG15 was taken from Crev-3 (Fig. 16C). All ice samples were of stratified ice of various colors and variable bubble content. The results are presented in Table 5.

Table 5. Otto Glacier δ2H and δ18O isotopic results*

Sample ID	UTM Easting	UTM Northing	δ^2H VSMOW ‰	δ^{18}O VSMOW ‰	Description
1BG15	12T 277138	4891465	-123.54	-16.05	Crev-1, 20 foot depth
2BG15	12T 277138	4891465	-130.06	-17.17	Crev-1, 30 foot depth
3BG15	12T 277061	4891586	-128.63	-16.97	Crev-2, 1 foot depth
4BG15	12T 276988	4891672	-128.96	-16.91	Crev-3, 3 foot depth
5BG15	12T 277087	4892276	-118.59	-16.31	meltwater pond

*Standard deviations for δ2H and δ18O are less than 1‰ and 0.2‰ respectively. Isotope ratios of δ 2H and δ18O are reported as ‰ values relative to the VSMOW2-SLAP2 scale.

The 2H and 18O isotopes data are of high quality, based on the accuracy and precision of the standards run with the samples. There is a small range between values. The lowest, or isotopically lighter, values are seen at the deepest ice depth in Crev-1 (-130 δ^2H, -17 δ^{18}O) while the heaviest values are seen in shallow ice and meltwater samples (1BG15 and 5BG15, respectively). This pattern may reflect a subtle warming in climate over the duration of years that is represented between the 10-foot-thick interval of stratified ice layers between samples 2BG15 and 1BG15. However, with such little change between only two data points this interpretation is inconclusive. It makes sense that the meltwater sample 5BG15 is on the heavier side of the observed range (-16.31) as the area had received rainfall in addition to snowfall in the weeks prior, thus likely mixing summer and winter isotopic compositions.

A comparison between Otto glacier data to δ^2H and δ^{18}O data from high mountain lakes in the Lemhi Range (Finney and Harrison, unpublished data) shows that the Otto isotopes are dominantly lighter than Lemhi Lake data (Fig. 20). This relationship supports the assumption that the Otto glacier is fed predominantly by isotopically lighter winter precipitation. The high mountain lakes in the Lemhi Range have isotopically heavier compositions due to the fact that they are fed by both snow meltwater and isotopically heavier summer rain. The isotopic compositions of the Lemhi Range lakes therefore

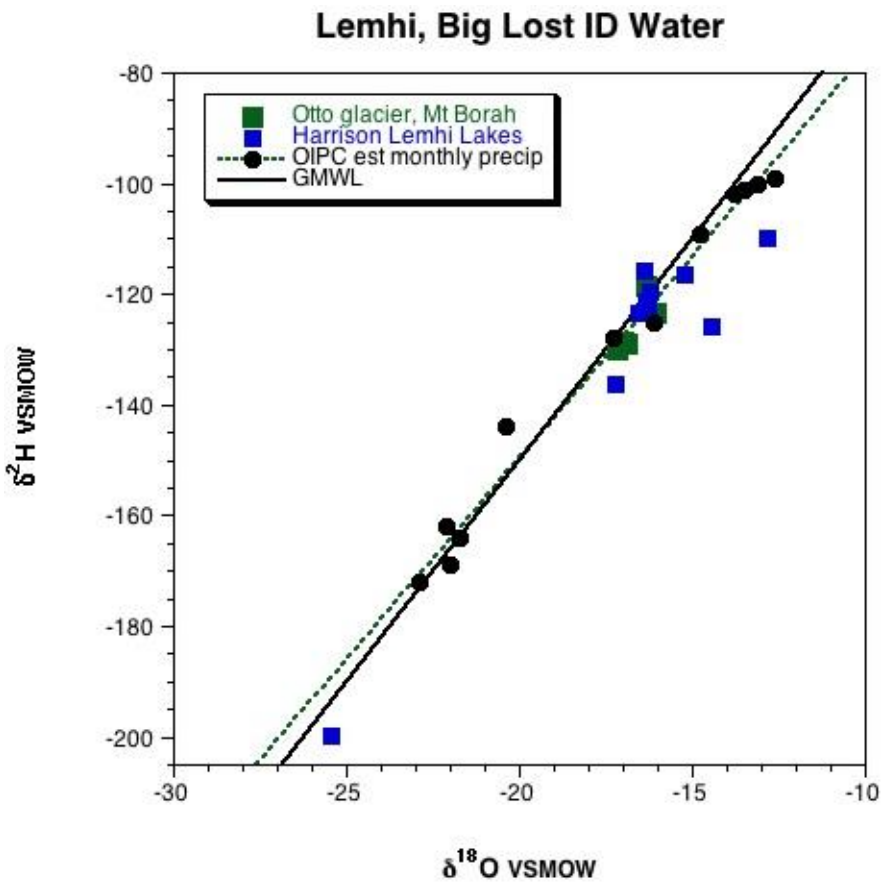

Figure 20. Plot showing δ2H and δ18O isotopic data for the Otto glacier and Lemhi Range lake samples along the Global Mean Water Line (GMWL). Estimated monthly values from the Online Isotope Precipitation Calculator (OIPC) show the expected isotope range significantly changes throughout the year (lower values in winter compared to summer).

presumably plot along a mixing line between light winter values and heavy summer rain values.

A recent study by Anderson et al. (*In Press*) shows that the isotopic composition of Rocky Mountain snowpack throughout Idaho, Montana and Wyoming, ranges between -17 $\delta^{18}O$ and -21 $\delta^{18}O$. Conversely, summer rain precipitation ranges between -5 $\delta^{18}O$ to -15 $\delta^{18}O$ (Gammons et al., 2006). The $\delta^{18}O$ data from Otto glacier is slightly heavier than the winter snow, and slightly lighter than the heaviest summer rain precipitation. This relationship is evidence for isotopic mixing between the two precipitation sources. One process that may skew isotopic compositions to be heavier than expected is winter snow removal by wind, which therefore reduces the amount of lighter isotopic compositions that are able to be made into glacial ice (Fisher et al., 1983). Another more likely process that leads to heavier compositions is the percolation of summer rain through the perennial snowpack, which partially

melts snow and ice and partitions heavier isotopic compositions into future glacial ice (Taylor et al., 2001; 2002).

In order to compare the Otto glacier isotopes with that of monthly precipitation observed in nearby Butte, MT, the Online Isotope Precipitation Calculator (OIPC) was used to estimate the isotopic values for the Borah Peak area. The OIPC is a tool that estimates the isotope ratios for any site and is based on a global dataset (Bowen, 2015). The comparison between the Otto glacier samples and monthly precipitation from Butte, MT (Gammons et al, 2006) shows considerable overlap (Fig. 21). However, looking only at late summer to fall data, when the Otto glacier was sampled, the plot shows that both the measured precipitation in Butte and the estimated OIPC values at Borah Peak are greater than what is observed in the ice. This further suggests that the isotopic values of the Otto Glacier are a product of isotopic mixing between winter and summer isotopic compositions.

Comparing δ^2H data between the Otto glacier and the Schoolhouse glacier in the Teton Range, we see an overlap in isotopic range and also that the Otto data is slightly heavier than what is observed from the Schoolroom glacier data (Finney, unbublished data) (Fig. 22). Comparing OIPC data from the Otto glacier, Schoolroom glacier and Fremont glacier (Wind River Range, WY), we again see close overlap with the Schoolroom and Otto glaciers. However, the Fremont glacier is estimated to be slightly lighter, perhaps due to its higher elevation of 13,300 feet, where as both the Otto and Schoolroom glaciers are about 10,400 feet.

2015 Climate

To best make sense of the hydrologic cycle as interpreted through the δ^2H and $\delta^{18}O$ data, and determine the dominant contributing climatic factors leading to the growth, recession and eventual preservation of the Otter glacier, comparison with past and present climate and weather trends is needed. To obtain weather data for the three nearby glaciers (Otto, Schoolroom, and Fremont), the online weather data calculator, PRISM, was used. PRISM calculates a weighted average based on triangulated data from nearby weather stations for any site. PRISM precipitation and mean minimum temperature for these three glaciers are shown in Figure 24. PRISM data for mean maximum temperatures is not shown because of the prominent similarities between all three glaciers.

The data show that temperatures and summer precipitation are highest at the Otto glacier location. The data indicate that without significant shading that the Otto glacier receives from the north face of Borah Peak, the glacier would likely have melted long ago due to the increased temperatures and melting effects of rainwater.

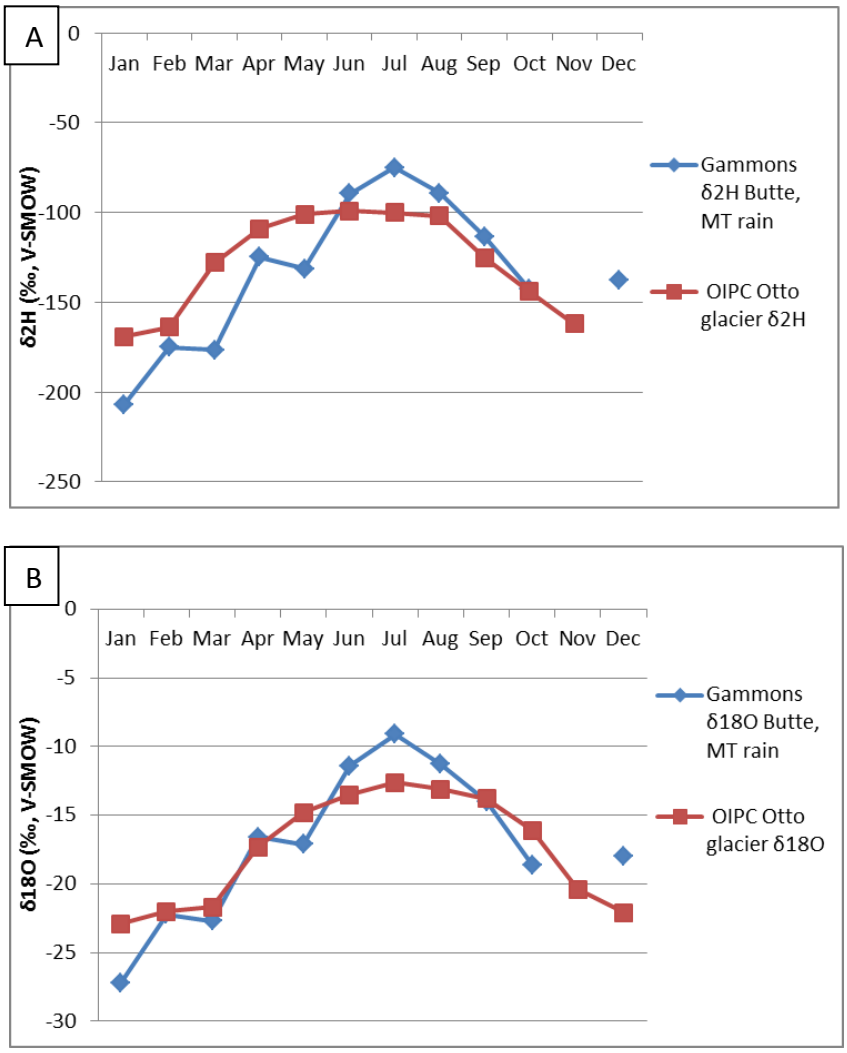

Figure 21. A: Plot showing monthly OIPC δ2H data for the Otto glacier with observed δ2H data from monthly precipitation at Butte, MT (Gammons et al, 2006). B: Plot showing monthly OIPC δ18O data for the Otto glacier with observed δ18O data from monthly precipitation at Butte, MT (Gammons et al, 2006).

RECOMMENDED STUDY

We recommend continued monitoring of the Borah Peak Glacier at the end of each ablation season usually between late August to early September. Relatively simple short-term and long-term studies would be inexpensive and would require few personnel. Reconnaissance surveying like the 2015 expedition is capable with little time and expenditure. Suggested annual monitoring includes surveying tips of crevasses, locations of visible stratified ice, tracking distinctive boulders on top of the moraine, and installing reference stakes across the glacier perpendicular to its flow direction. Precise GPS-aided surveys of these stakes and key features are needed to best quantify any cm-scale movement from year

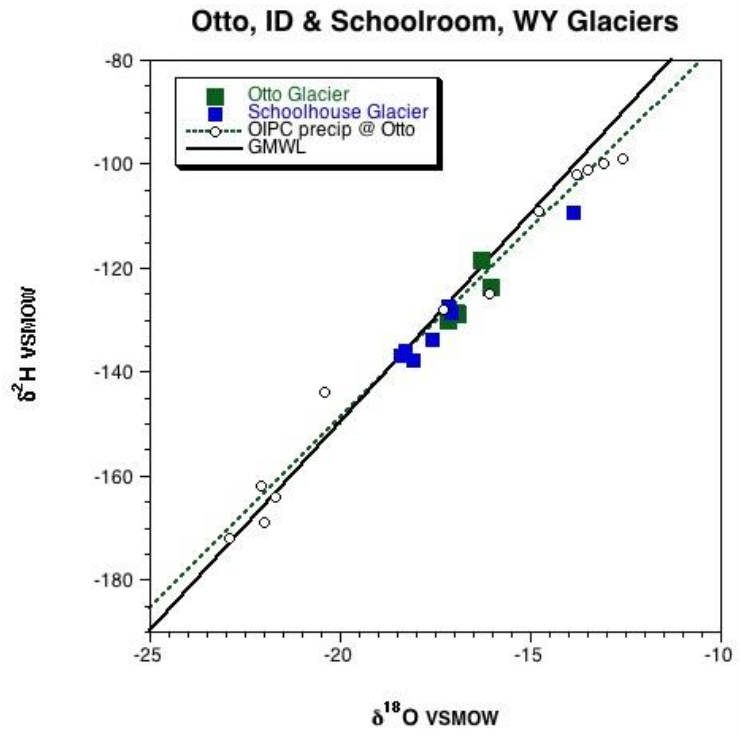

Figure 22. Plot showing δ2H isotopic data for the Otto and Schoolroom glaciers plotted along the Global Mean Water Line (GMWL) together with the predicted OIPC line for isotopic compositions at the Borah Peak area.

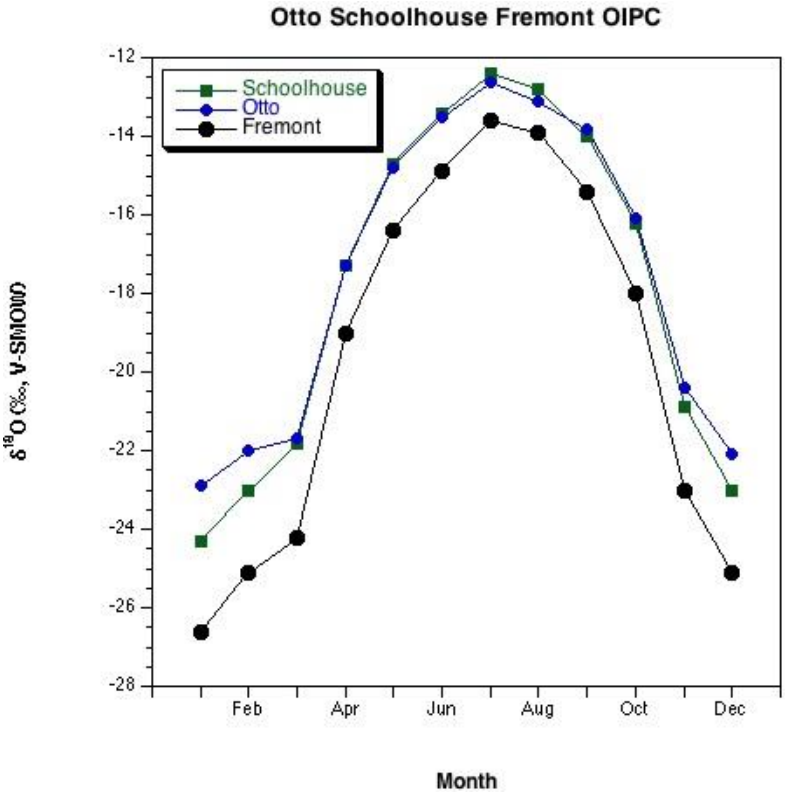

Figure 23. A: Plot showing monthly OIPC δ18O data for the Otto , Schoolroom and Fremont glaciers.

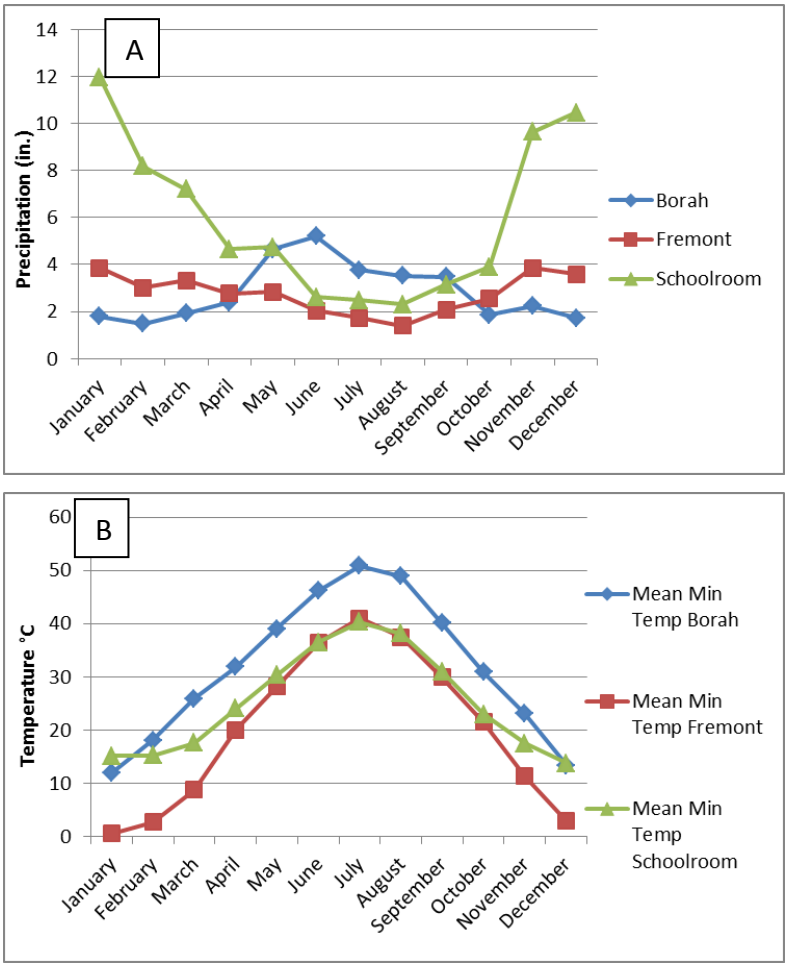

Figure 24. Plots showing PRISM-generated monthly weather data for the Otto , Schoolroom and Fremont glaciers. A: Monthly mean precipitation. B: Monthly mean minimum temperature.

to year. It is also recommended to make sure the stakes are durable enough to withstand intense bombardment from avalanches.

More intensive work would include drilling into the ice to obtain pristine ice samples at depth with less chance of contamination. Obtaining samples at depth would increase the likelihood of older ice, and further isotopic work on these would be useful. One geochemical marker used as an age proxy is radioactive isotope ^{36}Cl. Throughout the 1950-60's large amounts of ^{36}Cl were produced by fallout from atmospheric detonations of nuclear weapons (Davis and Schaeffer, 1955). In a 160-meter-thick ice core from the Upper Fremont Glacier in the Wind River Range, Wyoming, Cecil and Vogt (1997) measured a drop in ^{36}Cl below 32.0 meters, which was interpreted as a pre-nuclear-testing snow deposition based on the depth to tritium levels measured by previous workers.

The glacial history of Rock Creek and Otto glacier have high potential for further academic study as well. Established techniques using ^{10}Be on exposed bedrock can be used to track the glacier's recession to its present location. Tree ring analysis of trees in the upper portion of Rock Creek Cirque is another potential tool to track glacial regression.

As the isotopic work reported in this study is only a preliminary look into the hydrologic cycle in the Lost River Range, much more work can be done in this new and rapidly expanding field. We recommend comparing these results to the recently constructed meteoric waterline for southeast Idaho, Western Wyoming, and South-Central Montana (Benjamin et al., 2004).

CONCLUSIONS

The Otto glacier was discovered and determined to be an active glacier with a thickness of 64 meters in 1974 (Otto, 1975). Over the course of the next 41 years, eyewitnesses have established that the glacier's aerial extent and thickness have not changed very much since then. Our survey has confirmed the continued presence of the perennial ice mass originally identified in 1974, and concluded that the ice mass is indeed a glacier that continues to move under its own weight, based on measurements described herein in conjunction with results from the initial investigations in the 1970's. The glacier is classified as a semi-covered clean-ice glacier based on the thin surficial cover of rock debris over two-thirds of the glacier's extent. Total area from bergschrund crevasse to the toe-slope of the terminal moraine is 0.1 km^2 (25 acres). Remote sensing techniques using historical Google Earth imagery over a three-year period (2011-2014) has detected between 50 and 200 cm of *down*-slope movement per year. Although the geographic error within Google Earth imagery has been accounted for in this study, these measurements need to be precisely confirmed by GPS to solidify the evidence. Theoretical internal strain rates of the ice calculated using Glen-Nye flow law parameters independently predict velocities within this range but also overestimate what is observed at higher elevations and slopes. While the calculations offer a reasonable estimate of the rate of internal strain, many assumptions were used and may not actually reflect the conditions within the glacier.

Deuterium and oxygen isotopes were obtained from 4 ice samples and 1 meltwater pond downstream of the glacier. Delta deuterium (δ^2H) ranges from -130.06 to -118.59 VSMOW ‰ and $\delta^{18}O$ values range from -17.17 to -16.05 VSMOW ‰. A comparison between values and published snow and rain data from the northern Rocky Mountains, shows that the ice has integrated more positive summer precipitation with more negative winter precipitation. The processes that may have produced the isotopic mixing are winter snow removal by wind and/or percolation of summer rain through the

perennial snowpack. As this is only a reconnaissance effort, much more study and analysis of the data presented here is recommended.

ACKNOWLEDGEMENTS

This work was funded through the Watershed Monitoring Program at the Salmon-Challis National Forest thanks to lead hydrologist, David Deschaine. Thanks to Rebecca Arsenault for assistance in the field and to Mark Federman, Jeremy Powell, and Rick Schroeder for surveying assistance. Thanks to Bob Anderson of University of Colorado, Boulder, for discussions on modifying the Glen-Nye flow law. Thanks to Lawrence Kratz for mathematical assistance. Much thanks to Bruce Finney and Million Hailemichael for conducting isotopic analyses and providing expert interpretations. Thanks to Glenn Thackray and Mark Shapley for further discussion. Deep thanks to Bruce Otto and Collin Sloan for sharing their data from their initial and recent expeditions, and for their continued work and enthusiasm for the project, without which this work would not have been possible. Thanks also to Bruce Otto, Anne Kratz, and Jared Navratil for thorough reviews.

REFERENCES

Anderson, L., Berkelhammer, M., and Mast, M. A., *In Press*, Isotopes in North American Rocky Mountain Snowpack 1993-2014: Quaternary Science Reviews.

Benjamin, L., Knobel, L., Flint Hall, L., DeWayne, L., and Green, J., 2004, Development of a local meteoric waterline for southeast Idaho, Western Wyoming, and South-Central Montana: U.S. Geological Survey, Scientific Investigations Report 2004-5126, p 3-6.

Blackwelder, Eliot, 1915, Post-Cretaceous history of the mountains of central western Wyoming, Pt. 3: Journal of Geology, v. 23, p. 307-340.

Bloomfield, J.M., 1983, Volcanic ash in the White Cloud Peaks-Boulder Mountain region, south-central Idaho [M.S. thesis]: Bethlehem, Pennsylvania, Lehigh University, 136 p.

Bowen, G. J., 2015, The Online Isotopes in Precipitation Calculator, version 2.2. http://www.waterisotopes.org.

Cecil, L. D., and Vogt, S., 1997, Identification of bomb-produced chlorine-36 in mid-latitude glacial ice of North America: Nuclear Instruments and Methods in Physics Research Section B: Beam Interactions with Materials and Atoms, v. 123, no. 1, p. 287-289.

Clark, I., and P. Fritz., 1997, Environmental Isotopes in Hydrogeology: Lewis Publishers, Boca Raton, 328 p.

Colman, Steven M., and Kenneth L. Pierce, 1986, Glacial Sequence near McCall, Idaho: Weathering Rinds, Soil Development, Morphology, and Other Relative-age Criteria. Quaternary Research 25.1, p . 25-42.

Cotter, J.F.P., Bloomfield, J.M., and Evenson, E.B., 1986, Glacial and postglacial history of the White Cloud Peaks-Boulder Mountains, Idaho, U.S.A.: Geographie Physique et Quaternaire, v. XL, n. 3, p. 229-238.

Davis, R.J., Schaeler, O.A., 1955, Chlorine-36 in nature. Annals New York Academy of Science, v. 62, p. 105-122.

Fisher, D., Koerner, R., Paterson, W., Dansgaard, W., Gundestrup, N., and Reeh, N., 1983, Effect of wind scouring on climatic records from ice-core oxygen-isotope profiles: Nature, v. 301, p. 205-209.

Gammons, C. H., Poulson, S. R., Pellicori, D. A., Reed, P. J., Roesler, A. J., and Petrescu, E. M., 2006, The hydrogen and oxygen isotopic composition of precipitation, evaporated mine water, and river water in Montana, USA: Journal of Hydrology, v. 328, no. 1, p. 319-330.

Glen, J. W ., 1952, Experiments on the deformation of ice. Jourll. Glac., Vol. 2, No. 12, p. 111-I4.

Gosse, J. C., Klein, J., Lawn, B., Middleton, R., and Evenson, E., 1995, Beryllium-10 dating of the duration and retreat of the last Pinedale glacial sequence: Science, v. 268, no. 5215, p. 1329-1333.

Janke, J. R., Bellisario, A. C., and Ferrando, F. A., 2015, Classification of debris-covered glaciers and rock glaciers in the Andes of central Chile: Geomorphology, v. 241, p. 98-121.

Johnson, B. G., Thackray, G. D., and Van Kirk, R., 2007, The effect of topography, latitude, and lithology on rock glacier distribution in the Lemhi Range, central Idaho, USA: Geomorphology, v. 91, no. 1, p. 38-50.

Link, P. K., and Phoenix, E. C., 1996, Rocks, Rails and Trails (2nd ed.): Pocatello, Idaho, Idaho Museum of Natural History.

Luckman, B. H., 2000, The little ice age in the Canadian Rockies: Geomorphology, v. 32, no. 3, p. 357-384.

Nye, J. F. 1952, The mechanics of glacier flow: Journal of Glaciology, Vol. 2, No. 12, p. 82- 93.

Nye, J. F., 1965, The flow of a glacier in a channel of rectangular, elliptic or parabolic cross section. Journal of Glaciology, 5, p. 66190.

Ortiz, J., Guilderson, T., and Sarnthein, M., 2000, Coherent high-and low-latitude climate variability during the Holocene warm period: Science, v. 288, no. 5474, p. 2198-2202.

Otto, B.,R., 1975, Description of an Active Alpine Glacier, Lost River Range, Idaho.

Otto B.R. 1977, An Active Alpine Glacier, Lost River Range, Idaho: Northwest Geology.

Oakley, G. 1986, Otto's Glacier: Focus Magazine: Vol. XII, No. 1, Boise State University.

Pierce, Kenneth L., 2003, Pleistocene Glaciations of the Rocky Mountains. The Quaternary Period in the United States Developments in Quaternary Sciences (2003): 63-76.

Pierce, K. L., Obradovich, J. D., and Friedman, I., 1976, Obsidian hydration dating and correlation of Bull Lake and Pinedale glaciations near West Yellowstone, Montana: Geological Society of America Bulletin, v. 87, no. 5, p. 703-710.

Pierce, K. L., Licciardi, J. M., Krause, T. R., and Whitlock, C., 2014, Glacial and Quaternary geology of the northern Yellowstone area, Montana and Wyoming: Field Guides, v. 37, p. 189-203.

Reynolds, H. A., 2011, Recent Glacier Fluctuations In Grand Teton National Park, Wyoming [Master's thesis]: Pocatello, Idaho, Idaho State University, 215 p.

Taylor, S., Feng, X., Kirchner, J. W., Osterhuber, R., Klaue, B. r., and Renshaw, C. E., 2001, Isotopic evolution of a seasonal snowpack and its melt: Water Resources Research, v. 37, no. 3, p. 759-769.

Taylor, S., Feng, X., Williams, M., and McNamara, J., 2002, How isotopic fractionation of snowmelt affects hydrograph separation: Hydrological Processes, v. 16, no. 18, p. 3683-3690.

Thackray, G. D., Lundeen, K. A., and Borgert, J. A., 2004, Latest Pleistocene alpine glacier advances in the Sawtooth Mountains, Idaho, USA: reflections of mid latitude moisture transport at the close of the last glaciation: Geology, v. 32, no. 3, p. 225-228.